Powering Farm Autonomy with Green Energy

Achieving Agricultural Self-Sufficiency: A Swedish Case Study on Integrating Biomass, Photovoltaics, and Dual-Mode Energy Storage with Autonomous Electric Tractors on an Off-grid Farm.

Erik Guldevall

Master's Thesis, 30 credits

Swedish University of Agricultural Sciences, SLU

Faculty of Natural Resources and Agricultural Sciences, Department of Energy and Technology

Examensarbete (Institutionen för energi och teknik, SLU), 2026:7 • ISSN 1654–9392

M.Sc Energy System Engineering

Uppsala, 2026

Powering Farm Autonomy with Green Energy

- Achieving Agricultural Self-Sufficiency: A Swedish Case Study on Integrating Biomass, Photovoltaics, and Dual-Mode Energy Storage with Autonomous Electric Tractors on an Off-grid Farm.

Driva autonoma jordbruk med grön energi

- Att uppnå självförsörjande lantbruk: En svensk fallstudie om integrering av biomassa, solceller och dubbelverkande energilagring med autonoma eltraktorer på ett självförsörjande lantbruk.

Erik Guldevall

Supervisor:	Gunnar Larsson, SLU, Department of Energy and Technology
Examiner:	Åke Nordberg, SLU, Department of Energy and Technology
Subject reviewer:	David Ljungberg, SLU, Department of Energy and Technology

Credits:	30 credits
Level:	A2E
Course title:	Degree project in energy systems engineering
Course code:	EX1016
Program/education:	M.Sc Energy System Engineering
Course coordinating dept:	Department of Energy and Technology
Place of publication:	Uppsala
Year of publication:	2026
Cover picture:	Erik Guldevall
Copyright:	All featured images are used with permission from the copyright owner
Title of series:	Examensarbete (Institutionen för energi och teknik, SLU)
Part number:	2026:7
ISSN:	1654-9392

Keywords:	Self-sufficiency, Electric Tractors, Microgrid, Combined Heat and Power, Thermal Energy Storage, Battery Energy Storage, Photovoltaics, Pyrolysis, Biochar, Simulation, Carbon-Negative Agriculture

Swedish University of Agricultural Sciences
Faculty of Natural Resources and Agricultural Sciences
Department of Energy and Technology

Abstract

As the global agricultural sector faces increasing pressure to decarbonize and mitigate energy market volatility, transitioning from fossil-fuel-dependent machinery to electrified alternatives requires robust, autonomous on-site energy infrastructure. This thesis investigates the technical feasibility of achieving energy self-sufficiency on a Swedish wheat farm by integrating renewable generation with advanced energy storage systems. Specifically, the study evaluates a hybridized system comprising photovoltaic (PV) and biomass-driven Combined Heat and Power (CHP) generation with an Organic Rankine Cycle (ORC) combined with a dual-mode storage configuration: a 1 MWh Battery Energy Storage (BES) for short-term electrical balancing and a 20 MWh Molten Salt Thermal Energy Storage (TES) for long-term exergetic buffering. Additionally, the system utilizes pyrolysis for carbon sequestration and as a thermal energy sink.

A dynamic simulation model was developed in MATLAB/Simulink to analyze the system's performance over an annual cycle, with a specific focus on meeting the high-power charging demands of a fleet of autonomous electric tractors. The system's efficacy was evaluated using Key Performance Indicators (KPIs), including the Self-Sufficiency Ratio (SSR), State of Charge (SoC) dynamics, and Carbon Sequestering Ratio (CSR). The results demonstrate that the integrated configuration can achieve energy autonomy under baseline conditions and identify the 20 MWh TES as the critical component for system stability. In a comparative scenario in which the TES was removed, the SSR collapsed to 56.5% because the CHP's thermal output was treated as "wasted," and the inactive ORC engine was unable to mitigate fluctuations in electrical loads. Parametric sensitivity analyses revealed that biomass fuel quality and the CHP's operational efficiency are the primary technical bottlenecks governing the farm's energy balance. The findings suggest that while the transition to electric tractors is technically feasible through renewable integration, implementing high-capacity thermal storage is essential to provide the necessary flexibility for off-grid or weak-grid agricultural operations, but poses several technical challenges that require further inquiry. This research provides a framework for evaluating trade-offs between biomass storage, technical configurations, and system autonomy, offering a pathway to reduce the fossil-fuel dependency of modern food production.

Keywords: *Self-sufficiency, Electric Tractors, Microgrid, Combined Heat and Power, Thermal Energy Storage, Battery Energy Storage, Photovoltaics, Pyrolysis, Biochar, Simulation, Carbon-Negative Agriculture*

Executive Summery

This thesis investigates the technical feasibility of achieving complete energy self-sufficiency on a 200-hectare Swedish wheat farm as it transitions to autonomous electric machinery. Recognizing the agricultural sector's heavy reliance on fossil fuels and the resulting vulnerability to energy market volatility, the study evaluates an integrated off-grid microgrid powered entirely by locally sourced wheat-straw biomass and photovoltaic (PV) generation. To test this, a dynamic simulation model was developed using MATLAB/Simulink to analyze the farm's energy flows and fieldwork loads over a complete annual cycle. The proposed hybridized energy system features a biomass-driven Combined Heat and Power (CHP) generator and an Organic Rankine Cycle (ORC) engine, supported by a dual-mode storage configuration: a 1 MWh Battery Energy Storage (BES) for short-term electrical demands and a 20 MWh Molten Salt Thermal Energy Storage (TES) for long-term exergetic buffering. The system also integrates a pyrolyzer to process biomass byproducts into biochar, providing both a thermal energy sink and an environmental service through carbon sequestration.

The simulation results demonstrate that complete energy autonomy is technically achievable under baseline conditions, successfully maintaining a 100 % Self-Sufficiency Ratio (SSR) without requiring national grid support, even during the high-power charging spikes of the electric tractors. However, a comparative scenario analysis revealed that the 20 MWh TES is the most critical component for maintaining system stability. When the thermal storage was removed from the simulation, the farm's SSR collapsed to 56.5 %, proving that a large exergetic buffer is absolutely mandatory to decouple heat production from immediate electrical demand. Furthermore, parametric sensitivity tests identified the energy intensity of the biomass pelletization process and the nominal capacity of the CHP unit as the primary technical bottlenecks that can rapidly destabilize the microgrid if not carefully optimized.

Ultimately, while the research provides a successful proof of concept for a fossil-free, fully autonomous agricultural energy loop, the massive scale of the required storage infrastructure poses significant economic and practical challenges for an individual farmer. The findings confirm that implementing high-capacity thermal storage is essential for off-grid operations; however, adopting a hybrid approach, retaining grid connection to handle rare peak-load failures while maintaining a 95-98 % SSR, would likely offer a more resilient and financially viable pathway for modern farms aiming to decarbonize.

Populärvetenskaplig Sammanfattning

Detta examensarbete undersöker den tekniska genomförbarheten av att uppnå fullständig energisjälvförsörjning på en 200 hektar stor svensk veteodling som ställer om till autonoma elfordon. Med insikten att jordbrukssektorn är kraftigt beroende av fossila bränslen och därmed sårbar för volatilitet på energimarknaden, utvärderar studien ett integrerat off-grid-mikronät som drivs helt av lokalt producerad halmbiomassa och solcellsgenerering (PV). För att testa detta utvecklades en dynamisk simuleringsmodell i MATLAB/Simulink för att analysera gårdens energiflöden och arbetsbelastning under ett helt år. Det föreslagna hybrida energisystemet består av en biomassebaserad kraftvärmeanläggning (CHP) och en ORC-motor (Organic Rankine Cycle), kompletterat med två typer av energilagring: ett batterilager (BES) på 1 MWh för kortsiktiga elbehov och ett termiskt energilager (TES) med smält salt på 20 MWh för långsiktig exergetisk utjämning. Systemet integrerar även en pyrolysreaktor för att förädla restprodukter från biomassan till biokol, vilket ger både en termisk energisänka och en miljönytta genom koldioxidbindning.

Simuleringsresultaten visar att fullständig energisjälvförsörjning är tekniskt möjlig under basförhållanden, med en självförsörjningsgrad på 100 % utan behov av stöd från det nationella elnätet, även under de höga effekttoppar som uppstår vid laddning av eltraktorer. En jämförande scenarioanalys visade dock att 20 MWh TES är den mest kritiska komponenten för att upprätthålla systemstabiliteten. När det termiska lagret togs bort i simuleringen sjönk gårdens självförsörjningsgrad drastiskt till 56,5 %, vilket visar att en storskalig exergetisk buffert är absolut nödvändig för att frikoppla värmeproduktionen från det omedelbara elbehovet. Dessutom identifierade parametriska känslighetstester att energiintensiteten och kapaciteten i pelletsproduktionen samt kraftvärmeanläggningens nominella kapacitet är de främsta tekniska flaskhalsarna som snabbt kan destabilisera mikronätet om de inte optimeras noggrant.

Sammanfattningsvis ger forskningen ett konceptbevis för ett fossilfritt och helt autonomt energisystem för jordbruket. Den enorma omfattningen av den nödvändiga lagringsinfrastrukturen innebär dock betydande ekonomiska och praktiska utmaningar för en enskild lantbrukare. Resultaten bekräftar att implementering av termisk lagring med hög kapacitet är avgörande för off-grid-drift; att istället välja ett hybridupplägg, där man behåller en nätanslutning för att hantera sällsynta toppbelastningsproblem samtidigt som man bibehåller en självförsörjningsgrad på 95–98 %, skulle dock sannolikt erbjuda en mer resilient och ekonomiskt bärkraftig väg för moderna jordbruk som siktar på avkarbonisering.

Preface

With this master's thesis, I complete my educational journey toward a Master of Science in Energy System Engineering. This educational endeavor began far too many years ago with the intent of setting an academic foundation for my professional career, but it widened my perspective far beyond those boundaries. I now know that everything in this universe is a system of energy, and the wisdom I have gained over these years will forever guide me through life.

I had the opportunity to form my own thesis and recognized that one of the more important tasks today is to guarantee that the nodes of our civilization, humans, have the energy we need to propagate into the future. My formative years were defined by nature and technology, and as food security is increasingly compromised by climate change, energy scarcity, and ecological collapse, I knew that this thesis proposal from the Department of Energy and Technology at SLU fit my narrative. The scope was reconsidered many times, and though I would have wanted to focus more on the nature aspect of the system developed, I do hope this read provides you with a glimpse into what agriculture could become. Regenerative and self-sustaining.

For inquiries regarding the thesis or subjects discussed, please contact: erik.guldevall@gmail.com

Erik Guldevall
Uppsala, April 2026

Contents

List of tables

List of figures

List of equations

Nomenclature

BE: Biological energy (Bioenergy)
TES: Thermal Energy Storage
BES: Battery Energy Storage
KPI: Key performance indicator
SoC: State of Charge
CSR: Carbon Sequestering Ratio
SSR: Self-Sufficiency Ratio
ECL: Energy Control Logic

1 Introduction

In this first chapter, the thesis's motivation is presented. The purpose, research questions, and outline of the report follow.

In the 21st century, a transformative era unfolds, marked by global challenges such as population growth, rising energy demand, and the impacts of climate change. Amidst these towering challenges, the agricultural sector is responsible for fueling the main actors and heralds of our global society, us humans. Contemporary agrarian practices rely heavily on fossil fuels for machinery and to derive artificial fertilizers; however, this access is finite and harms our environment, so we must adapt. At the heart of this mission of adaptation is an energy paradigm: how we produce our food and the electricity we need, without having to source them from elsewhere that might need it as much as we do.

As our societies adopt more technology across all sectors, even the contemporary farm becomes increasingly intertwined with the digital age and will soon partially rely on autonomous electric machinery and sensor-based systems. This thesis builds on studies conducted at the Swedish University of Agricultural Sciences on the use of electric tractors in Nordic climates [26,27]. While enhancing efficiency and yields, this technological surge brings about a substantial shift in the energy dynamics of these systems, which must adhere to the conventions of diverting from fossil fuels and degenerative practices. Recognizing the need for transformation, this exploration, guided by the author, delves into the pivotal role of readily available local energy sources and alternative storage solutions in building a reliable, flexible energy infrastructure for the unfolding new agricultural situation.

Specifically, this thesis investigates the technical feasibility of achieving complete energy self-sufficiency on a Swedish wheat farm by utilizing a closed-loop microgrid. By integrating photovoltaic (PV) generation with a biomass-driven Combined Heat and Power (CHP) unit fueled by locally sourced wheat straw pellets, the system aims to meet all internal energy demands. To manage the high-power charging spikes of autonomous electric tractors and bridge seasonal gaps in renewable generation, the study evaluates a dual-mode storage configuration. This includes a Battery Energy Storage (BES) system for short-term electrical balancing and a Molten Salt Thermal Energy Storage (TES) unit coupled with an Organic Rankine Cycle (ORC) engine for long-term exergetic buffering. Furthermore, the system incorporates a pyrolyzer to process biomass byproducts into biochar, providing both a thermal energy sink and an environmental service through carbon sequestration. Through dynamic computer modeling in MATLAB/Simulink, this thesis seeks to identify system bottlenecks, test hardware configurations, and ultimately determine whether an off-grid, carbon-negative agricultural model is a viable pathway to secure our future food production

1.1 Purpose

This thesis investigates the feasibility of a Swedish wheat farm meeting all its energy demands by utilizing locally sourced biomass and photovoltaic energy, supported by long- and short-term thermal and electrical energy storage systems. To achieve this, the primary purpose is to construct a computer simulation model of the farm's overall energy requirements, specifically accounting for the integration of electric tractors. This model is then subjected to variable-parameter configurations to assess operational self-sufficiency using the simulated data. By evaluating these scenarios to identify critical system requirements, technical bottlenecks, and areas for improvement, this research aims to provide an overview and valuable insights for future projects focused on off-grid or power-producing renewable food production.

1.2 Questions

The following research questions are intended to be answered in the thesis.

1. Can a Swedish wheat farm be self-sufficient in electricity, utilizing only photovoltaics and locally sourced wheat straw?

2. Does heat energy storage improve the energy self-sufficiency of the farm, and to what extent compared to one without it?

3. Which components can cause bottlenecks within the energy system, and can they be reasonably adjusted to address these issues?

4. What and how much byproducts are produced, and how can they be utilized to perform environmental services?

1.3 Outline of the Report

This report explores agricultural energy autonomy across several structured chapters. The Introduction establishes the motivation for off-grid renewables and outlines the core research questions regarding biomass and solar energy feasibility, while the Background contextualizes global climate challenges and the farming sector's need to shift away from fossil fuels.

To ground the study, the Theory chapter details the underlying software, equipment, and concepts. Building on this, the Methodology describes the research approach, detailing the MATLAB/Simulink 200-hectare farm model, data collection, and Key Performance Indicators (KPIs) like the Self-Sufficiency Ratio (SSR).

The Results chapter delivers simulation data addressing the research questions across three scenarios. Through visualizations of energy storage levels and electrothermal flows, it analyzes system performance and includes a parameter configuration sweep that identifies bottlenecks like pelletizer energy intensity and CHP capacity.

Finally, the Discussion analyzes these findings and their broader implications, while the Conclusion explicitly answers the research questions and summarizes technical feasibility, followed by Further Studies with recommendations for future research.

2 Background

This chapter introduces the reader to the circumstances the author considered when choosing the thesis and its subjects.

2.1 Fossil-Fuel dependency

Despite Sweden’s fossil-free sources generating approximately 98.5% of its electricity in 2023 [1], the country’s overall energy landscape remains a complex mix, with the agricultural sector still significantly fossil-fuel-dependent. While the stationary components of the Swedish economy, such as district heating for housing and industrial production, have largely decoupled from carbon-intensive sources, the fuel required for field operations in agriculture and logistics is still overwhelmingly supplied by fossil diesel [1]. In Swedish farms, fuel consumption for machinery has remained remarkably stagnant over the last three decades. While emissions from heating agricultural buildings have plummeted from 0.5 million tonnes CO_2-eq in 1990 to roughly 0.1 million tonnes in 2020 due to the adoption of heat pumps and biomass boilers, emissions from internal combustion engines in equipment have remained at approximately 0.4 to 0.6 million tonnes CO^2-eq annually [2]. This indicates that the agricultural sector remains tethered to fossil-fuel infrastructure, despite trends in other sectors. This dependency creates a severe systemic vulnerability, making the Swedish food supply chain highly sensitive to price volatility in the global oil market. Events such as the 2022 energy crisis or the current situation in the Strait of Hormuz, precipitated by geopolitical instability, demonstrate that a sudden spike in diesel prices directly threatens farmers' profitability and, by extension, Sweden's national food security. Because most Swedish agricultural machinery utilizes diesel cycles and rejects other liquid fuels except HVO, farmers lack immediate flexibility when diesel prices rise [3]. Replacements such as HVO are viable but have been shown to track fossil-fuel product prices [4].

Furthermore, the centralized nature of fossil fuel distribution makes Swedish farms susceptible to logistical disruptions. In a crisis scenario, the interruption of oil imports would effectively paralyze the national food production system within weeks, as gas stations and delivery trucks cease to function amid a choked energy infrastructure. Transitioning to a decentralized, autonomous electric energy system derived from locally sourced biomass and photovoltaics is, therefore, not only an environmental objective but also a critical strategy for increasing the resilience of Swedish agriculture. Decoupling from external supply dependencies while maintaining, or even increasing, productivity would be the ultimate success story for agriculture in the 21st century.

2.2 Straw as Fuel

In the pursuit of agricultural autonomy and decoupling from the fossil fuel market, grain straw represents a readily available bioenergy (BE) carrier that is often underutilized. The almost exclusive use of grain is as food for humans while the straw is utilized as roughage, low quality fodder for animals, simply left on the fields or in some cases combusted for energy. Of all commonly grown grains, wheat straw is highly suitable for energy production due to its abundance, renewability, and favorable chemical composition. As an agricultural byproduct, wheat straw is widely available, accounting for around 20 % of agricultural biomass in Europe [5]. It contains 30–40 % cellulose, 20–30 % hemicellulose, and 15–20 % lignin, components that contribute to its high calorific value of 14–17 MJ/kg [5]. In the Uppland region, where wheat is a dominant crop, the energy yield per hectare is substantial and, when processed, can be used to pursue farm energy self-sufficiency. Traditionally, straw’s low bulk density hinders its use as a fuel in conventional systems, leading to logistical inefficiencies and combustion challenges [6].

2.2.1 Harvest

The harvesting of wheat straw involves a few sequential steps after the residual straw is left, followed by the separation of wheat grain. The process begins with a combine harvester, which cuts the wheat crop, threshes the grain, and separates it from the chaff and straw. The straw is discharged from the back of the combine in rows, referred to as windrows, to prepare it for later use [9]. Once the operator windrows the straw, baling equipment compresses it into dense, uniform bales for easy transport and storage. The baling process demands precise moisture management; farmers typically bale the straw when moisture levels fall below 15 % to prevent microbial activity and mold from damaging the crop [10]. High moisture levels promote conditions conducive to fungal proliferation, which degrades the quality of the straw by consuming its organic material and reducing its energy potential. Additionally, excessive moisture can cause heating in storage systems, further accelerating deterioration and reducing its quality as a BE feedstock [10]. Under certain conditions, this can even lead to spontaneous combustion.

Following baling, the straw is loaded onto trailers for direct transport and stored in on-site, covered conditions before being delivered to the farm's energy conversion facility. Proper storage of wheat straw is essential to maintain its quality. The key factors influencing wheat straw storage include moisture control, environmental conditions, and protection against biological and physical deterioration. Storage facilities must protect straws from rain and humidity. Covered barns, warehouses, or plastic wraps can effectively prevent moisture infiltration. Plastic wrapping also provides UV protection and helps minimize straw decomposition caused by sunlight. Ventilated airflow around bales prevents moisture accumulation and damp spots that encourage mold growth. The storage space allows for adequate circulation without exposing straws to outdoor elements. Temperature should remain below 25°C to minimize biological activity and reduce the risk of spontaneous heating [11]. In hot climates, shaded or insulated storage can prevent excessive heat buildup within bales.

2.2.2 Pelletization

Pelletization converts wheat straw into a high-quality bioenergy feedstock by compressing straw into a 0,5-2 mm radius pellet [7], with a maximum size of 5 mm [8]. The moisture content is then reduced to an optimal level of 5–15 % to prevent clogging during compression and increase pellet durability [7]. The reduced moisture content is essential for achieving high combustion efficiency in end-use applications. The system feeds the processed straw into a pellet mill, which applies high pressure and moderate heat (typically 70–90 °C) to the material [9]. Under these conditions, the natural lignin present in wheat straw softens and acts as a binding agent, reducing the need for external additives [9]. Pelletization addresses challenges such as bulkiness, low energy density, and handling difficulties associated with raw straw. Pellets of uniform size and moisture content promote consistent combustion, resulting in higher energy efficiency and lower particulate emissions. The compact pellet form allows them to be used in automated feeding systems for both small- and large-scale biomass boilers (CHP), enhancing operational convenience.

Unfortunately, straw is a complex fuel. Unlike woody biomass, as mentioned at the beginning of the chapter, it contains high levels of alkali. These contents can lower the ash melting point, potentially leading to slagging and fouling in standard combustion chambers. The pelletization process homogenizes the fuel, increasing its energy density and potentially providing the stable combustion temperatures required to curtail slagging effects of lower combustion temperatures. Further refinement of the pellets into biochar additionally alleviates slagging effects by removing much of the problematic contents of the original straw fuel and providing exceptionally cleaner and higher-temperature combustion [10].

The transformation of wheat straw into bio-energy also mitigates the environmental harm associated with leaving straw residues on fields. In conventional agricultural practices, portions of the straw are left as field residue and decompose under both aerobic and anaerobic conditions, such as when the straw is submerged in wet soil, which is common during Swedish harvest seasons. This process emits both carbon dioxide (CO_2) and methane (CH_4), potent greenhouse gases that contribute to agricultural sector emissions and exacerbate global warming [11]. Collecting and utilizing straw in bioenergy systems curtails carbon and methane emissions and repurposes the carbon stored in the straw for energy, CO^2 sequestration, and soil improvement.

2.2.3 Handling

Wheat straw pellets also require careful management to maintain quality, prevent degradation, and ensure safe handling over time. The moisture content of pellets needs to be below 10-12 % to avoid microbial growth and decomposition [12]. Proper ventilation is necessary to prevent condensation and heat accumulation, while stored pellets should remain at a stable temperature below 40°C to avoid spontaneous combustion [13]. Additionally, mechanical stability is crucial to minimize breakage and dust formation. Indoor storage is preferred as it protects against precipitation and humidity fluctuations. For large-scale storage, silos offer a more compact and efficient option. Metal or reinforced concrete silos provide structural integrity and prevent moisture infiltration, while built-in ventilation systems help maintain uniform temperature and humidity levels. Real-time monitoring sensors can detect temperature spikes or increased CO_2 levels that indicate potential degradation [13]. Humidity control also requires the use of dehumidifiers or moisture-absorbing materials. Additionally, pre-treatment methods such as coating pellets with hydrophobic substances or adding natural binders can improve their resistance to moisture absorption [14].

2.2.4 Energy Carrier

A common critique of removing straw from fields is the potential depletion of soil organic carbon and nutrients [15]. To mitigate this, farmers are integrating circular exergy models, meaning the system becomes more energetically efficient by reintegrating byproducts to a greater extent, thereby optimizing the useful electric/heat energy (Exergy) produced. In this framework, the process retains the straw’s biological exergetic functions rather than consuming and losing them; instead, it partitions the straw's energy, carbon, and mineral content. The system combusts the pellet fuel to produce electric and thermal energy. It directs a portion of that thermal energy to stabilize the carbon in the pellets through pyrolysis, ultimately returning the resulting ash and biochar to the fields. This approach preserves the nutrient loop while utilizing the carbon as an energy carrier. By harvesting straw, the farm effectively captures its summer solar gain in a physical, storable form and dispatches it during the high-demand winter months when PV output drops in Swedish latitudes.

2.2.5 Other Uses

Wheat straw is also sometimes used as animal feed, particularly in regions where other feed resources are limited. However, it is considered a low-quality forage due to its low crude protein of around 3.6 %, which is lower than barley (4.1 %) and oat (4.5 %) straw, and its high lignin and cellulose levels, which reduce digestibility, do not provide sufficient nutrition for proper growth or lactation [16]. To improve its nutritional value, it is often treated with chemicals (e.g., ammonia) or supplemented with higher-quality feed, and is more common in mixed rations or during fodder shortages [16]. Farmers primarily use straw as bedding material or roughage, though they can easily substitute it with other agricultural residual straws. Given its availability, high energy content, and low nutritional value, wheat straw is a more practical option for bioenergy production.

2.3 Dual Energy Storage combined with Green Energy

2.3.1 Thermal Energy Storage

Long-term Thermal Energy Storage (TES) is a useful technology for balancing energy supply and demand in renewable energy systems. It allows excess thermal energy to be stored and used when needed, improving efficiency and reliability in power generation and industrial applications. Its effectiveness is determined by the physical mechanism used to store energy. These technologies are generally categorized into three primary types. Hot liquid and solid, also known as "Sensible", heat storage is the most mature and widely implemented approach, involving the storage of energy by heating a storage medium, such as water, rocks, or molten salts, without undergoing a phase change [17]. The total energy capacity is determined by the material's specific heat capacity and the temperature gradient. Latent heat storage uses Phase Change Materials (PCMs) to absorb or release energy during a phase change, typically between solid and liquid states. Because these materials maintain a nearly constant temperature during phase change, they offer a high energy density, making them ideal for regulating battery temperature in electronics, and are almost exclusively used in small applications [18]. Finally, thermochemical storage represents the most advanced, high-density category, utilizing reversible chemical reactions to store and release energy. Because energy is stored as chemical potential rather than heat or physical form, it can be held indefinitely at ambient temperatures without thermal loss. While currently the least commercially mature, thermochemical systems offer the highest potential for long-duration energy security in decentralized systems [19].

To achieve agricultural autonomy in the Swedish climate, a system must manage two distinct energy vectors: electricity for mechanical work (tractors) and farm processes, such as pelletizing and space climatization, and heat for pelletization. The integration of Photovoltaics (PV) and a wheat pellet-fueled Combined Heat and Power (CHP) unit with Thermal Energy Storage (TES), Battery Energy Storage (BES), and Organic Rankine Cycle (ORC) engines provides the necessary thermodynamic functions to bridge the gap between intermittent renewable generation and fluctuating farm demand for various energy forms (Electric, Heat, Solid fuel). Due to climate degradation and extreme weather fluctuations, a system that handles and processes readily available nearby biomass is more resilient than one that cannot produce electricity and needs a connection to the grid. The amount and type of fuel to grow, along with system dimensions, can be adjusted to suit other locations with other prerequisites.

2.3.2 Combined Heat and Power

In a Combined Heat and Power (CHP) configuration, the engine converts a portion of the biomass's thermal energy from the combustion into high-grade electricity. At the same time, the remaining waste heat is captured through a heat exchanger and delivered to thermal loads. This dual output is the cornerstone of the system's efficiency, maximizing the chemical energy in the straw. Given the high temperatures required for effective CHP operation, molten salt or high-temperature oil systems are often the standard for industrial-scale applications. In conventional farming, heat and electricity are often treated as separate streams: grid electricity and heat from a standalone boiler. A CHP system unifies these streams. This unification is essential to creating a system that performs a broader range of functions without becoming overly complex or undesirable to adopters.

2.3.3 Organic Rankine Cycle

The Organic Rankine Cycle (ORC) unit uses an organic fluid with a lower boiling point than water to generate electricity from low- to medium-temperature heat sources. The process involves heating the fluid until it evaporates, expanding the high-pressure vapor through a turbine to drive a generator, and then condensing the fluid back into a liquid to repeat the cycle [20]. Unlike internal combustion engines, the ORC engine is driven by an external heat source. In a farm-scale bioenergy system, an ORC engine is a reliable and efficient means of converting stored thermal energy into electrical power. In traditional systems, ORC engines are directly coupled to the combustion chamber; in this design, the TES serves as an intermediate thermal reservoir. This offers several operational advantages, including the ability to smooth fluctuations in combustion output, extend operating hours beyond active combustion, and optimize energy dispatch in response to electricity demand. ORC engines are also characterized by high reliability and the ability to operate continuously at steady state [21], which would provide an appreciated peak-shaving service to a system solely reliant on PV and CHP. An ORC-upgraded CHP system enables the farm to generate its own base-load electricity precisely when demand is highest, curtail heat for long-term storage and peak shaving, creating an energy flow that reduces reliance on the external grid during peak demand.

2.3.4 Photovoltaics

Modern photovoltaics (PV) modules used in agricultural applications typically consist of monocrystalline or polycrystalline silicon cells, offering conversion efficiencies of ground-level solar irradience to electric energy, of 17 % - 22 % under standard test conditions [22]. Recent advancements in panel design and surface coatings have further improved low-light performance and durability, making PV a viable solution even in northern climates like Sweden, where seasonal irradiance can vary substantially. The integration of PV with the farm's microgrid and BES systems supports load balancing, particularly during daytime operations such as machinery charging. Surplus electricity generated during peak sunlight hours can be stored directly in BES, curtailed to the TES via a heater, or fed into the national grid, enabling both energy independence and revenue generation through feed-in tariffs or power purchase agreements during high-demand, low-yield hours. Because energy production from PV does not always align with energy consumption (driven by tractor charging and weather), a buffer is required. BES handles short-term electrical spikes, and TES handles long-term energy management while utilizing otherwise wasted energy.

2.4 Carbon Sequestration

While burning wheat straw provides immediate thermal and electrical energy, it also produces harmful exhaust emissions. A sophisticated way to compensate for this is to create biochar through Pyrolysis, a thermochemical decomposition of organic material at elevated temperatures (300-600 °C) in the absence of oxygen [23]. The process has two byproducts: syngas and biochar. Syngas is a mixture of hydrogen and carbon monoxide, with varying amounts of carbon dioxide and methane [23]. In a decentralized farm energy system, pyrolysis produces biochar that can be utilized as a carbon neutral fuel or to sequester carbon for negative emissions. Unlike the natural decomposition of straw on the field, which, as established in Section 2.1, releases CO_2 and CH_4, pyrolysis locks the atmospheric carbon captured by the wheat during its growth into a refined, carbon-rich form that can be returned to the soil. Biochar can remain stable in the soil for centuries, effectively acting as a greenhouse gas and soil biology stabilizer [24]. By incorporating pyrolysis into the farm's energy cycle, the system could transition to carbon-negative status, directly mitigating the agricultural sector's greenhouse gas footprint.

Beyond carbon sequestration, applying biochar to Swedish soils (which often experience compaction and nutrient leaching) offers regenerative benefits. Biochar increases the soil's cation exchange capacity and water-holding capacity, potentially reducing the need for fossil-fuel-intensive synthetic fertilizers [25]. This creates a regenerative feedback loop: the energy system powers the electric tractors that deliver the necessary wheat byproduct, which fuels energy production, enhancing the land's productivity and resilience.

3 Theory

This chapter begins with a visual overview of the developed system in Figure 1 to give the reader a framework of components used in the study, introduces the theoretical material that constructs the components, and the scientific concepts behind them. Firstly, the reader is informed of the autonomous electric tractor thesis that forms the basis for the construction of the Simulink model used in this thesis, and subsequently explain all system components

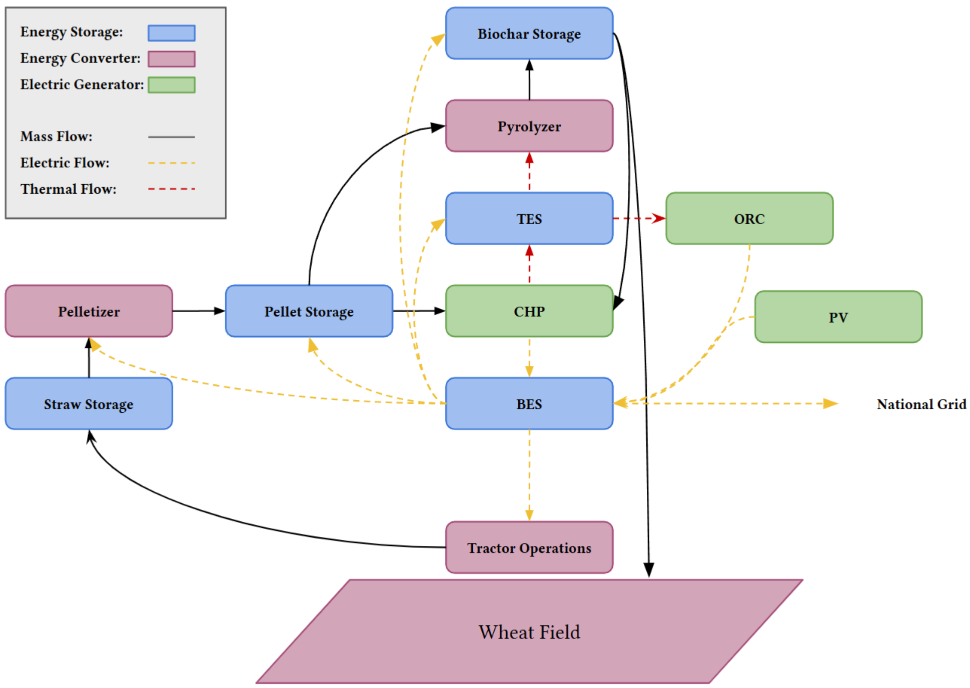

Figure 1: A visual overview of the system to provide an understanding of the component setup and energy flows between them.

3.1 The Tractor Fieldwork Simulink Model

The foundation of the entire master's thesis is based on previous studies by PhD Oscar Lagnelöv at the Swedish University of Agriculture regarding electric tractors, their optimal energy systems, and working conditions in the Swedish environment [26]. The models developed simulate various field parameters using historical weather data and tractor behavior. The result is an overview of the acceptable working hours of electric tractors on the farm and an estimate of their behavior, including the electrical load on the tractor engine, charging, and battery swapping during operation. The electric tractors are based on the base configuration provided in Lagerlöv's 2019 report [27] and utilize the same Simulink model. In the report, two types of battery systems for tractors are described: one with conductive charging, where the tractor docks and charges at a fixed position, and one that charges the batteries and replaces them with depleted ones in tractors returning from operation. The latter was determined to be superior, as it provided the most versatile and efficient charging, leaving less time for the tractors to idle without work or to have readily charged batteries. The battery exchange configuration used in the study to model tractors' charging behavior consists of two tractors with a 50 kWh battery capacity each, one additional battery, and one charger dock with a 50 kW charging power. Further details on the tractor fieldwork model are available in the sources [26,27].

3.2 Pelletizer

Energy consumption to knife/hammer-mill wheat straw into particles of the desired size varies noticeably depending on the method used. For knife- and hammermills, wheat straw reduction to about 1,5 mm radian particles requires 7,5 and 37 kWh/t, respectively [28]. The pelletization of wheat straw cuttings consumes about 153 kWh/t, according to research by Niedziółka and Szpryngiel at the University of Life Sciences in Lublin [29]. However, this number is dramatically lower when reviewing options on the commercial market where pelletization machines perform as low as 60, 55, and even 22 kWh/t [30–32]. This drastic difference can be explained by the different methods used in micro-scale lab environments versus macro-scale industrial environments, leading to varying pellet quality, properties, and power performance, which affect system performance and the handling of pellet fuel.

3.3 CHP

A Pellet Combined Heat and Power Generator, also known as a cogeneration system, is a technology that generates electricity and utilizes the waste heat from biomass, in this case, wheat pellets derived from the farm's agricultural byproducts. This dual-output process significantly improves overall fuel efficiency compared to separate heat and power production. While conventional power plants typically achieve total efficiencies of 40–50 %, CHP systems can exceed 80 %, depending on configuration and operating conditions [33]. In this study, the selected CHP unit is designed for biomass pellet combustion, supporting the integration of renewable energy within decentralized energy systems.

Figure 2 below shows a simple overview of the CHP and energy storage setup. The system consists of a biomass-fired boiler, a gas turbine connected to the BES, and a heat recovery system connected to the TES. The CHP generator used in the study is modeled after the specifications of a Fröling fixed-bed gasifier with an electric capacity of 56 kW, a thermal capacity of 115 kW, and a pellet consumption of 40 kg/h, assuming a moisture content of less than 10 % [34]. For simplicity, it is assumed that all thermal energy is delivered to the TES without losses. This, of course, is a huge oversight, as the heat-transfer capabilities of the exchangers from the CHP to the TES are temperature-dependent, and the required exchangers would have to operate at unrealistic efficiencies. Meaning: energy is more efficiently allocated between a hot and a cold medium; in this case, both CHP and TES will at times have temperatures close to the same, drastically reducing energy delivered to the TES. This must absolutely be taken into account when considering the realism of the system. However, a recent study from late 2025 in China suggests that a CHP system combined with molten-salt TES shows promising results for exergy improvements, but for power-generating systems of much larger magnitude [35]. For the sake of innovation, the author decided to allow this incongruity in the system configuration.

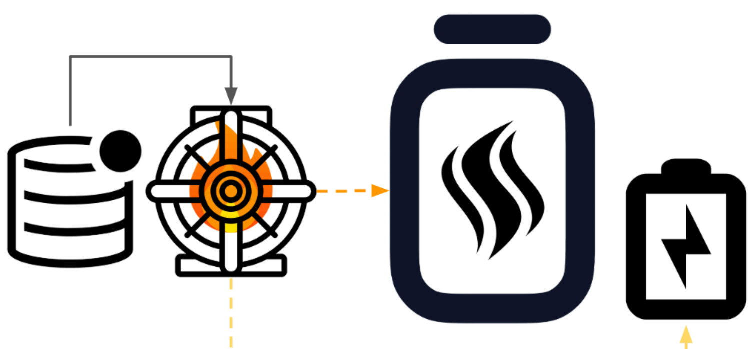

Figure 2: CHP Setup, Pellets are fed to a boiler connected CHP generator. Produced Electric energy is fed to the BES and Thermal energy to the TES.

3.4 BES

The electric battery storage used in the thesis consists of two subsystems: Three 50 kWh tractor batteries and a large BES with a 1 MWh capacity for intermediate energy storage in the farm-wide energy system. Both systems consist of lithium-ion battery modules, and the BES is configured to deliver a nominal power output of up to 100 kW over a 10-hour discharge duration. However, most battery management systems prevent batteries from reaching 0 % to protect their health and usually set a Depth of Discharge (DoD) around 10 % [36], resulting in a discharge duration of 9 hours, which is assumed in this thesis for the BES. Cycle-life degradation refers to the gradual loss of a battery's maximum energy capacity and the increase in its internal resistance, caused by the chemical and physical wear of repeated charging and discharging. As the lithium-ion cells age, they fundamentally lose the ability to store and deliver the same amount of power [37]. Cycle-life degradation is not considered for any of the batteries used, but it should be included to better capture system behavior over the system's lifetime.

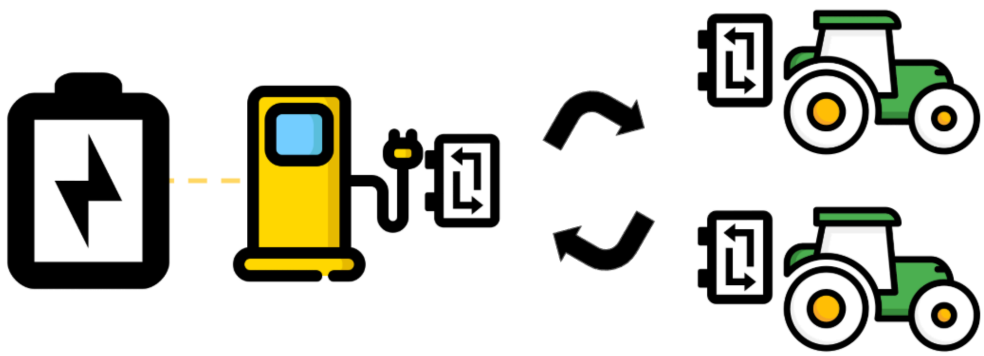

Figure 3: The electric battery setup. Two batteries power the electric tractors, while the third is charged with power available from the BES.

3.5 TES

Among the various TES methods evaluated during model development, molten salt heat storage was found to be well-suited due to its high thermal stability, cost-effectiveness, scalability, and compatibility with a high-temperature pyrolyzer. Molten salt-based TES is widely used in various industrial applications and typically consists of a mixture of sodium nitrate ($NaNO_3$) and potassium nitrate (KNO_3), which serves as a high-capacity heat storage medium with a specific heat capacity (c_p): about 1,5 kJ/kg·K, and the ability to operate at temperatures between 250°C and 600°C [38]. All thermal flows between the TES and other components, such as the ORC engine and Pyrolizer, are assumed to occur without losses.

Because the TES considered in this thesis operates at high temperatures, a loss coefficient was developed to account for thermal losses to the environment, given its likely relevance to the system's performance. To minimize thermal losses through the shell, a common and effective high-temperature insulator is rockwool. This material can achieve a thermal conductivity coefficient of approximately k ≈ 0.09 W/m·K at temperatures between 250 and 600°C [39]. Below are the calculations required to assess the steady-state heat losses through the shell of a cylindrical TES, and Figure 4 shows the schematics of the insulation shell. Ambient temperature data is provided by SMHI (Sveriges meteorologiska och hydrologiska institut).

$$\frac{dQ_{total}}{dt} = \frac{d}{dt}\left(\pi k (T_{salt} - T_{ambient})\left[\frac{2L}{\ln(r_2/r_1)} + \frac{2(r_2-r_1)^2}{r_2-r_1}\right]\right) \qquad (1)$$

Eq 1: Thermal losses through the TES shell [40]. r_1 and r_2 refer to the inner (storage medium tank) and outer (storage medium tank and insulation) radius, i.e., Δr is the thickness of the insulating medium of 1 m. Typically, the bottom of TES rests on another medium of different thickness; It is assumed that all surfaces are equally insulated.

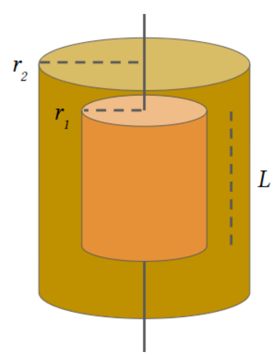

Figure 4: TES insulation schematics

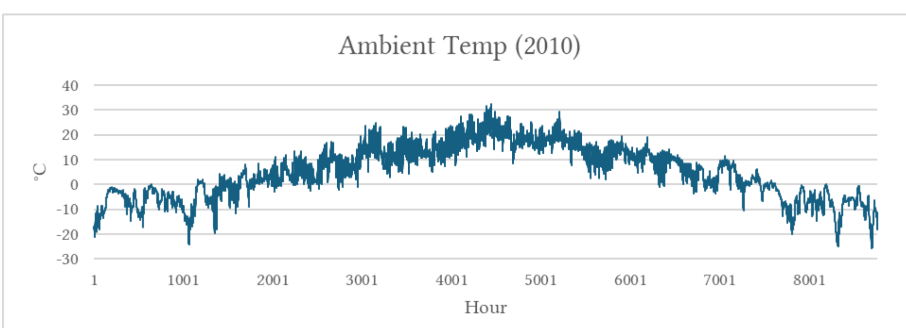

Figure 5: Ambient temperature (SMHI)

3.6 PV

A typical Swedish barn roof offers ample surface area for PV installation, with an estimated 600 m² or more, sufficient to host 40–80 kW of installed PV capacity, depending on orientation, tilt, and local insolation levels [41]. Below are the calculations provided for the solar array utilized in this case farm. The solar irradiance consists of hourly values (W/m^2) from a location just outside Uppsala (Latitude: 59.757, Longitude: 17.693) provided by SMHI [42], and calculated based on an array with a tilt of 41°, south-facing—data using the European Commission tool PGIS (Photovoltaic Geographic Information System) [43].

$$P = A \cdot G \cdot \eta \qquad [2]$$

Eq 2: PV output (Power) as a function of Area (A), Solar irradiance (G), and Conversion efficiency (η)

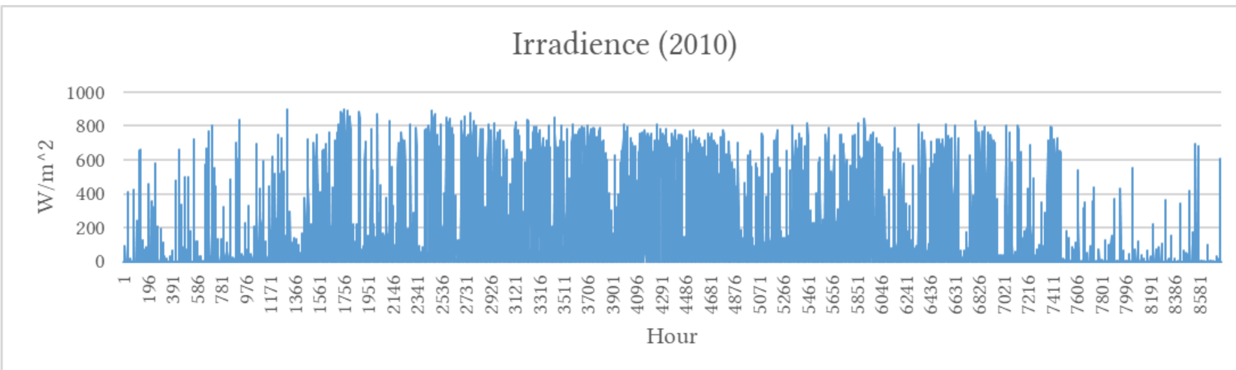

Figure 6: Solar irradiance data (SMHI)

3.8 ORC Engine

The ORC engine (Figure 5) receives thermal energy from a heat exchanger connected to the molten-salt TES. The heat is transferred to the evaporator, where it vaporizes the working fluid, initiating the thermodynamic cycle. The ORC engine converts this thermal gradient into mechanical work by expanding the high-pressure vapor through a turbine or screw expander, which then drives a generator that produces electricity. This electricity is fed directly into the BES, enabling flexible energy use to power farm operations, charge electric tractors, or supply surplus power to the grid. The efficiency of ORC engines depends on the temperatures of the storage medium and the ambient air, which, in this case, is the outside temperature provided by SMHI [42]. Below is the efficiency equation for this system's ORC engine.

$$\eta_{ORC} = 1 - \frac{T_{Environment}}{T_{TES}} \quad (3)$$

Eq. 3: Efficiency of ORC engines

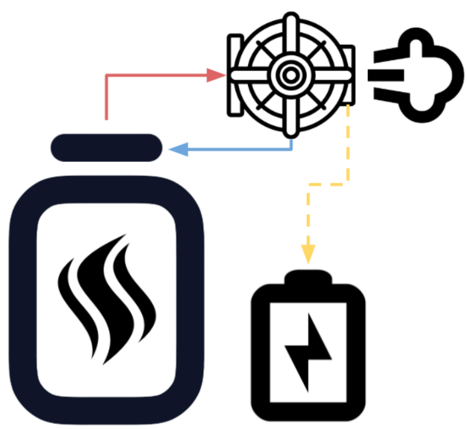

Figure 7: The ORC engine setup

3.9 Storage Climatization

Finding exact data on the energy requirements of equipment used in wood/straw pellet storage facilities for climatization was difficult, so the author made some assumptions. The peak self-heating power of wood pellets at 30°C is 0.04 W/kg due to decomposition [13]. To mitigate heat buildup in large silos, this energy must be removed from the storage environment through refrigeration and also ventilation of the latent moisture trapped during the pellet production. Assuming a coefficient of performance of 3 for refrigeration, and an additional load of 25 % for ventilation (ϕ), conservatively [44,45]. The climatization of the storage therefore uses a parasitic load proportional to the mass stored and is calculated using equation 4 below.

$$P_{total} = m_{pellet/char} \cdot P_{ref.} \cdot \left(\frac{1}{COP} + \phi\right) \qquad (4)$$

Eq 4: Biomass storage climate control load

3.10 Pyrolyzer

Pyrolysis is the thermochemical decomposition of organic matter through the application of heat in an oxygen-deficient environment. Unlike combustion, which is a fully oxidizing process, pyrolysis partitions the chemical energy of biomass into three distinct categories: solid carbonaceous residue (biochar), condensable liquid (bio-oil), and non-condensable syngas [46]. Product partitioning is primarily governed by operating temperature and heating rate. Pyrolysis is classified into five primary types based on operating temperatures and rates to maximize specific energy output. Slow pyrolysis heats biomass slowly over hours or days at moderate temperatures to maximize solid, carbon-rich biochar production. Intermediate pyrolysis serves as a bridge, using moderate heating rates and residence times of 10 to 30 minutes to achieve a balanced, uniform yield of biochar, bio-oil, and syngas. To maximize liquids, fast pyrolysis heats biomass for under two seconds, then instantly cools the vapors to produce up to 75 % liquid bio-oil, while flash pyrolysis takes this mechanism further by using micro-particles and ultra-short residence times (<0.5 seconds) to produce highly refined bio-oils or light gases. Finally, high-temperature pyrolysis bypasses solids and liquids entirely by operating above 800°C to crack heavy molecules into permanent, non-condensable syngas. For this study, "Slow pyrolysis" is considered the preferred method, as it maximizes the yield of stable biochar for carbon sequestering [47]. For many pyrolysis systems, the produced syngas is repurposed to fuel the thermal reaction (quasi-autothermal) or to power external generators; these functions drastically lower the external energy input and should be investigated, but are outside the scope of this study, along with the syngas byproducts, to simplify the theory of this component. In the simulation modeling, pyrolysis is approximated as requiring 2.88 MJ/kg (0.8 kWh/kg) of total energy to produce biochar from wheat pellets, resulting in a 70 % mass reduction and yielding 0.3 kg of biochar per kg of wheat pellets [48].

4 Methodology

This chapter begins with a brief description of the methodology and the Key Performance Indicators used to evaluate the resulting data. Followed by a description of the system along with a review of the parameters of system components and their values in the Baseline model and the Energy Control Logic that controls them. Finally, a description of the three scenarios the model is put through during simulation.

This study applies a quantitative systems analysis methodology combining dynamic computer-based energy system modeling, scenario analysis, and feasibility assessments to evaluate the technical viability of achieving complete energy self-sufficiency for a Swedish wheat farm. Utilizing local biomass (BE) and photovoltaic (PV) generation supported by a dual-mode storage configuration—comprising a short-term Battery Energy Storage (BES) system and a long-term Thermal Energy Storage (TES) unit—the farm-wide architecture is simulated using MATLAB/Simulink (SimEvents). This software framework enables a detailed, time-dependent evaluation of electro-thermal energy flows, storage state-of-charge dynamics, and seasonal environmental variability. Furthermore, systematic sensitivity analyses are performed to identify critical operational parameters and technical bottlenecks, which are paired with a complementary qualitative assessment to explore regenerative agricultural benefits, such as carbon sequestration via biochar production, and the overall system integration with localized food production.

The methodological process begins with a system definition phase, during which the farm's boundaries, components, and energy flows are established. The system includes electricity and heat demands, PV generation, biomass energy conversion, and both electrical and thermal storage components. Empirical and literature-based data are collected for key parameters, including thermal and electrical battery parameters, component conversion efficiencies, storage characteristics, and system parasitic loads. All assumptions are explicitly stated to ensure transparency and reproducibility. The simulation model developed in MATLAB's Simulink enables temporal analysis of energy flows, storage saturation, energy storage SoC, system input, and output at hourly and seasonal resolutions. The model is used to analyze three case scenarios and test different configurations and operational strategies. These scenarios are evaluated using performance indicators: self-sufficiency, energy storage SoC, and carbon sequestration ratio.

4.1 Analysis methods

To evaluate the case and answer the research questions, four KPIs are used to process the quantified data produced by the Simulink model: Self-sufficiency, State of Charge, Carbon Sequestering Ratio, and Biomass Balance.

4.1.1 Self-sufficiency Ratio (SSR)

Systems involving PV arrays commonly use the Self-Sufficiency ratio concept [49], but in this case, wheat pellets and CHP also provide energy. SSR refers to the proportion of the system's energy demands that can be met by internal energy production. In this specific case, the demands are not compared to energy production but rather to whether the system requires energy supplied by the national grid (i.e., an external energy source). The total yearly internal energy production ($E_{produced}$) is compared with the amount supplied by the grid (E_{grid}), and the difference must fall within a certain margin; for this study, that margin is less than 1 % to achieve self.sufficience, leaving 1 % for simulation errors. See Equation 5 below:

$$SSR = 1 - \frac{E_{grid}}{E_{produced}} < 0,01 \quad (5)$$

4.1.2 State of Charge (SoC)

This concept usually refers to the battery's charge level; in this case, it is interesting to examine how much electrical energy the BES (Eq. 6, 7 below) and thermal energy TES (Eq. 8, 9 below) has available at different points in time. By examining how often or for how long the State of Charge falls below a threshold, energy excess or deficiency can be evaluated for a given system configuration. For example, over the course of a year (h_{year}), hours with SoC below/above X% can be quantified and studied. In this case, the interesting SoC for the BES is the number of hours it falls below 10 % (*h,SoC<10*, energy deficit) and above 95 % (*h,SoC>95*, energy excess). For the TES, the lower-threshold measure (energy deficit) needs to be adjusted to account for the energy required to keep the TES above freezing (≳ 250 °C), which corresponds to an SoC of about 42 %. The lower threshold for the TES is therefore set to SoC < 55 % to maintain a realistic margin during periods of heavy thermal discharge.

$$BES, SoC < 10 = \frac{h,SoC<10}{h_{year}} \quad (6) \qquad BES, SoC > 95 = \frac{h,SoC>95}{h_{year}} \quad (7)$$

$$TES, SoC < 55 = \frac{h,SoC<55}{h_{year}} \quad (8) \qquad TES, SoC > 95 = \frac{h,SoC>95}{h_{year}} \quad (9)$$

4.1.3 Carbon Sequestering Ratio (CSR)

One of the aims of the thesis is to design a system that is as carbon-neutral or even carbon-positive as possible. It is therefore worth investigating the fate of the carbon captured by the wheat fields. Ideally, the system should sequester the maximum amount of carbon with the least energy possible, balancing the energy invested in sequestered carbon. This can be determined by measuring the energy input to the system (E_{in}) and the biochar produced ($m_{biochar}$). These two are then compared to obtain an applied energy ratio per unit mass of biochar across all the different system configurations to be simulated. See eq. 10 below.

$$CSR = \frac{E_{in}}{m_{biochar}} \quad (10)$$

4.1.4 Biomass balance

Given biochar's ecological and economic value, it is important to evaluate the system's ability to process the fields' biomass produced during the year by measuring the stored straw and biochar at the end of the simulated period. This measure simply highlights whether any system configuration more efficiently utilizes the input biomass to produce valuable output. It also provides some insight into how the BE is distributed.

4.2 Definition of the case study

The following segment shortly describes the system studied from the wheat field to biochar.

The studied case is a 200-ha wheat farm located in Uppsala, Sweden, in 2010. It used two autonomous electric tractors for all field operations and harvested its crops at the end of the summer season, leaving straw residue for energy production. The straw is cut and delivered to an initial storage area of unspecified size, where it is fed to a pelletizer, turning straw into pellets that are delivered to silos of unspecified size, but conditioned by climatizers whose electric load is proportional to the amount of stored pellets. These pellets then fuel a CHP generator, which serves as the main energy producer for the farm-wide energy system, along with a 200 m^2 PV array, and feeds its electric output to a BES and its thermal output to a TES. The BES provides the tractors, pellet storage, biochar storage, and pelletizer with the required electrical power. Excess energy produced when the BES SoC reaches 100 % is routed to the TES via a heater. The TES, in turn, has two major functions: to deliver heat for the pyrolysis of pellets into biochar and to produce electricity through an ORC engine when the TES's SoC approach 100 %.

4.3 Case Study Descriptions

In this segment, Table 1 shows all system baseline parameters, followed by brief descriptions of the system components and the values that define them in the Simulink model.

Table 1: Technical Simulation Parameters, Baseline Configuration

Component	Parameter	Value	Unit
Wheat Harvest	Harvest yield	4018	*kg/ha*
PV Array	Peak Capacity (200m^2)	80	kW_R
	Efficiency (η)	0.2	*%*
CHP Units	Electrical Output (P_e)	56	*kW*
	Thermal Output (P_{th})	112	*kW*
	Fuel Consumption	40	*kg/h*
ORC Engines	Rated Power	50	*kW*
	Thermal- to electric (η)	25-30	*%*
Tractor Dock Charger	Charging Power	95	*kW*
	Battery Capacity	50	*kWh*
BES	Total Capacity	1000	*kWh*
	Max Charge Rate/Discharge Rate	250	*kW*
TES	Storage Capacity	20 000	*kWh*
	Operational Temp	250 - 600	*°C*
	Heat loss coefficient	12	*W/K*
Pelletizer	Production/Consumption	500	*kg/h*
	Electric Consumption	16,75	*kW*
Climate control	Electric Consumption	0,1	*W/kg*
Pyrolyzer	Heat Consumption	137	*kW*
	Pellet Consumption	167	*kg/h*
	Char Production	50	*kg/h*
Heater	El. to Heat	100	*kW*

4.3.1 Technical Baseline Simulation Parameters

To ensure the reliability and reproducibility of the Simulink model, the technical parameters for each subsystem are derived from manufacturer specifications, empirical agricultural data, and established thermodynamic constants. These parameters define the physical constraints of the energy system. The selection of these values reflects a "state-of-the-art" Swedish wheat farm, assuming the integration of high-efficiency monocrystalline photovoltaics and professional-grade biomass gasification technology. By grounding the model in these specific technical data points, the simulation can accurately calculate the hourly energy balances and identify the precise moments where supply-side generation meets or fails to meet the high-power demands of an electrified autonomous tractor fleet. During the development of the Simulink model, a Baseline component configuration evolved and served as the base from which all simulations were derived. Table 1 below presents the parameters and their respective values, based on the best available technology and data from the literature, to achieve the set goals.

4.3.2 Wheat field and Tractor

The field has an area of 200 ha and yields 4018 kg of wheat straw per ha, which is the mean over the years 2017-2023 [33], multiplied by the above-ground residue ratio for wheat grain-harvest of 0.7 [50]. Further information on tractor behavior can be found in previous studies [26,27].

4.3.3 Biomass Storages

All biomass storage is assumed to be unlimited in size to allow for the theoretical utilization of all wheat straw produced. The main focus is to investigate the energy system, and optimal storage sizes could be derived using the produced data, which justifies not predetermining their size. Pellet and biochar storage include a parasitic climatization load of 0.0232 W/kg,h for ventilation and dehumidification, proportional to the stored mass. However, because these storage capacities are unlimited, this value is rounded up to 0.1 W/kg to align with the larger ventilation penalties required for hypothetically very large storage areas. This would also include some of the electrical loads required to dry the straw and pellets at the various stages mentioned in the literature.

4.3.4 Pelletizer and Pyrolyzer

The pelletizer consumes 16.75 kW/500 kg, with the same mass of straw going in as the mass of pellets out. For the pyrolyzer, as discussed in section 3.9, it is assumed that it consumes 0.8 kWh to process 1 kg of pellets into 0.3 kg of biochar. From this, derive the baseline pyrolyzer capacity of 167 kg/h of pellets, producing 50 kg of biochar at a heat load of 137 kW, based on a Spanish pilot biochar plant [48].

4.3.5 CHP and PV

The CHP design is a simple binary on/off system that consumes 40 kg/h of pellets and produces 56 kW of electrical energy and 112 kW of thermal energy, based on the German Fröling CHP generator [34]. The CHP uses values for wood chips instead of wheat pellets, which have different attributes; the exact power input/output may differ.

In the hybrid energy system outlined in this thesis, PV arrays play a complementary role by providing daytime electrical generation, especially during peak solar periods, at a relatively low investment cost. PV power production is proportional to the array area (baseline 200 m^2), the array efficiency (0.2) [43], and the solar irradiance data from a weather station in Stockholm in 2010, provided by SMHI [42].

4.3.6 ORC Engine

In the baseline Simulink model, there is one ORC engine using Eq 3 and internal data for the TES medium temperature, along with the ambient temperature provided by SMHI, to calculate its efficiency, rated at 50 kW.

4.3.5 Energy Storages

The only parameters for the BES are its 1 MWh storage capacity and a Max Charge/Discharge Rate of 250 kW. The TES dimensional parameters are required to calculate its thermal losses to the environment. While creating the Simulink model, several capacities were tested, and the baseline was set to 20 MWh. The storage medium operates between 250-600 °C, which means that the available energy that can safely be extracted from the TES without it freezing is about 10 MWh (SoC at 50 %, ca 300°C).

A 20 MWh Salt TES is noticeably larger than industry standards and housed in a cylindrical tank about 5 m in diameter (r_1= 2.5 m) and 5 m in height (L), optimized for minimal surface area and reduced heat loss through the shell. For insulation, the TES uses rockwool, a commonly used material for industrial insulation that can withstand the temperatures of the molten salt, with a heat transfer coefficient $k \approx =$ 0.09 W/m·K.

In the model, the thickness of the insulation is assumed to be 1 m ($r_2 - r_1 =$ 1 m), which is considerably large, but deemed necessary to keep thermal losses low. Eq. 11 (Based on Eq 1, section 3.5) below is used in the Simulink model and calculates heat loss through the TES shell to the environment as a function of the TES size, insulation thickness and the temperature difference between the tank salt (T_{salt}), calculated internally in the model, and the ambient temperature ($T_{ambient}$), from environmental data provided by SMHI.

$$Q_{total} = \pi k(T_{salt} - T_{ambient})[\frac{2L}{ln(r_2/r_1)} + \frac{2(r_2-r_1)^2}{r_2-r_1}] \approx 12\, W/K \qquad (11)$$

Eq 11: TES Thermal loss calculation. K is the thermal transfer coefficient of Rockwool, T_{Salt} The temperature of the salt medium, $T_{ambient}$: The ambient temperature, r_1:The radius of the TES tank (2,5 m), and r_2: which is r_1 (2,5 m) + Rockwool insulation (1 m) = 3,5 m.

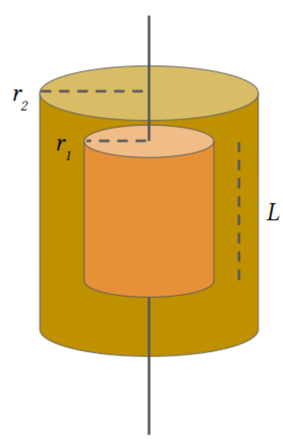

Figure 4: TES insulation schematic

4.4 Energy Control Logic

The operational heart of the Simulink model is the Energy Control Logic, which dictates the power flow between generation sources, storage units, and the farm's electrical and thermal loads. In the model, these states are set within "charts" that define their functions based on external conditions. Example: "CHP is on if pellets are available and BES SoC is below X". To maintain the BES and TES within a functional range while prioritizing renewable self-sufficiency, a hierarchical dispatch logic is implemented. The system operates in a state-dependent control loop, where the SoC of the BES and TES, and BE fuel availability serves as the primary trigger for power/heat generation.

The dispatch priority is programmed as follows:

1. **Photovoltaic:**
   As the most direct and carbon-neutral source, solar power is top-prioritized for energy supply to the BES. Because it cannot store captured energy elsewhere, it requires available capacity in the BES at all times, as reflected in the Energy Control Logic, which gives PV precedence over all other electric sources.

2. **ORC Engine:**
   To reduce mechanical wear in the biomass combustion system, the model first seeks to bridge electric energy deficits using stored thermal energy. If the BES SoC falls below 50 %, the ORC engine is activated, provided the TES maintains a thermal SoC above 95 % to supply energy for an extended period without freezing the storage medium and causing damage. This way, previously stored waste heat generates electricity without requiring immediate pellet combustion, effectively shaving the load peak.

3. **CHP:**
   When the BES SoC falls below a critical threshold of 10 %, and the TES SoC is insufficient to power the ORC engine, the CHP unit is engaged. The system verifies fuel availability before initiating the combustion cycle and remains active until the BES SoC reaches 99 % or the TES reaches 100 %. A secondary logic is applied similarly to provide heat to the TES if its SoC falls below 50 %, again to prevent freezing.

4. **Grid supply:**
   The final tier of the logic is an emergency safety net to prevent deep discharge and potential system blackout. If the BES SoC drops below 5 %, indicating that solar, thermal, and biomass resources collectively cannot meet demand, the farm draws power from the national grid. This event is recorded as a failure in self-sufficiency, and the cumulative energy drawn here is used to calculate the final SSR for the scenarios.

5. **Heater:**
   Due to its lower capacity and tendency to reach maximum SoC, the BES funnels excess energy to the TES via a direct electric heater. This allows PV power supplied to the BES at SoC 100 % to remain in the ES, preventing BES overload.

Table 2 on the next page provides exact operating ranges and conditions for all system components, including the pelletizer and pyrolyzer.

Table 2: Energy Control Logic

Component	State	BES SoC (%)	TES SoC (%)	Pellet Storage (kg)	Straw (kg)
CHP	On	< 10		> 10	
			< 50	> 10	
			< 62.5	> 50 000	
	Off	>= 99			
			>=100		
				< 1	
ORC	On	< 50	> 95		
	Off	>= 99			
			< 55		
Heater	On	> 99			
	Off	< 99			
Grid charge	On	< 5			
	Off	> 5			
Pelletizer	On			< 55 000	> 10
	Off				= 0
				>= 75 000	
Pyrolyzer	On		> 62.5	> 49 000	
	Off		< 50		
				< 49 000	
PV	On	Always			

Table 2: For the On/Off state to be triggered, each condition on a row must be met. For some components there are several sets of conditions that can trigger a state. In the first two rows: The "On" state of the CHP for example can be triggered if BES SoC falls below 10 % and there is more than 10 kg (> 10) of pellets in storage, or if the TES SoC falls below 50 % and there is more than 10 kg of pellets in storage. Only one row of conditions need to be met to trigger a state for a component.

4.6 Scenario Descriptions

The following segments describe the 3 scenarios designed to answer the study's research questions. Scenario 1-3 aims to produce the conditions required to answer questions 1-3, respectively.

4.6.1 Scenario 1 (Baseline Configuration)

The first scenario serves as the baseline for the entire study. It is designed to answer the primary research question: *Can a Swedish wheat farm be self-sufficient in electricity, utilizing only photovoltaics and locally sourced biomass?* This scenario establishes the technical feasibility of the proposed off-grid system under standard operational conditions for the 200-hectare wheat farm in the Uppsala region. In this scenario, the farm is modeled as a closed energy loop. The system boundary is strictly defined to exclude any continuous support from the national grid, with a success threshold defined as a Self-Sufficiency Ratio (SSR) of 99 %. The simulation utilizes a 1-hour time step over a full meteorological year (8,760 hours). This resolution is selected to capture the high-power "spikes" caused by the 95 kW charging of electric tractors' exchangeable batteries, and to compare them against simultaneous generation from the PV array and the 56 kW CHP units. The model is populated with the data described in sections 4.3-4.5.

The methodology for this scenario involves an annual simulation of the entire system. By analyzing periods when the SoC is at its lowest, and the SSR is high, the simulation determines whether the current CHP and BES sizing is sufficient to bridge the dark period of the Swedish winter, when PV contribution is negligible, and the post-harvest period, when pyrolyzer load is at its peak. The results of Scenario 1 provide the benchmark against which the subsequent TES-enhanced and byproduct-optimized scenarios are compared.

4.6.2 Scenario 2 (Non-TES)

Scenario 2 transitions from the system's basic feasibility to a focused optimization study of its thermal components. While the farm's primary goal is electrical self-sufficiency, integrating a high-temperature TES creates a hybrid energy buffer that decouples heat production from immediate electricity demand. The purpose of this scenario is to answer the second question of the thesis: *Does heat energy storage improve the energy self-sufficiency of the farm, and to what extent compared to one without it?* And to quantify the resilience and environmental gain provided by stored thermal energy. The analysis in Scenario 2 employs a comparative "With vs. Without" methodology. The simulation is executed using the same 8,760-hour meteorological dataset (SMHI/PVGIS) and the same tractor fieldwork load profiles as used during testing of scenario 1. However, it excludes all thermal functions associated with the TES, including the ORC engine. In this mode, the ORC engine is deactivated when the TES is absent. The CHP (115 kW) heat output is treated as a waste that cannot be converted back into electricity. All high-power events, such as the 95 kW tractor charging spikes, pyrolys, which are now fueled by electric input of the same magnitude (137 kW) as the previous thermal from the TES, and a 16.75 kW pelletizer. All must be covered exclusively by the 1 MWh BES, the 80 kW-rated PV array, or the active 56 kW CHPs, as needed.

This configuration is then compared with the results from scenario 1, and the analysis focuses on the *SSR*, *SoC* drift, and R_C. By overlaying the BES SOC curves from both configurations, the study identifies critical intervention points: moments when the ORC engine prevents the battery from falling into the emergency grid charge zone (BES SoC < 5 %).

4.6.3 Scenario 3 (Parametric Sweep)

While the previous scenarios establish the general feasibility and the role of TES, Scenario 3 investigates the mechanical and operational limits of the farm’s converter hardware. In a complex energy system, self-sufficiency is often limited not by a lack of raw resources (straw or sunlight), but by "chokepoints", components whose rated capacities are insufficient to handle peak energy flows. This scenario seeks to identify these bottlenecks and propose "reasonable adjustments" to the system architecture to achieve the 99 % self-sufficiency target. The primary objective of Scenario 3 is to answer the third research question: *What components cause bottleneck effects, and how can they be adjusted?* The hypothesis is that the high-power demand of the 95 kW electric tractor charging docks will create a transient deficit that cannot always be met by a single 56 kW CHP unit, even with battery support. By incrementally increasing the converters' capacity, the study identifies the optimal "hardware balance" for a 200-hectare operation.

To systematically identify bottlenecks in the farm’s energy system, a series of parametric sweeps is conducted. By varying the rated capacity of one hardware component while holding all others at their baseline values, the simulation can isolate the sensitivity of the Self-Sufficiency Ratio (SSR) to specific mechanical constraints. The configurations listed in Table 3 (below) show the "stress-test" matrix. Each category (A through E) addresses a distinct hypothesis about system limitations during peak-demand or low-resource periods.

Table 3: Parametric Sweep Configurations, Scenario 3

Config.	CHP (kW) (115 kW heat)	ORC (kW)	Pelletizer (kW/500kg,h)	Pyrolyzer (kg/h)	PV Area (m^2)
A.1 (Baseline)	56 (112 kW Heat)	50	16,75	50	200
A.2	28 (56 kW Heat)	50	16,75	50	200
A.3	112 (224 kW Heat)	50	16,75	50	200
B.1	56	25	16,75	50	200
B.2	56	75	16,75	50	200
C.1	56	50	11	50	200
C.2	56	50	27,5	50	200
C.3	56	50	33	50	200
C.4	56	50	76,5	50	200
D.1	56	50	16,75	25	200
D.2	56	50	16,75	75	200
E.1	56	50	16,75	50	0
E.2	56	50	16,75	50	400
E.3	56	50	16.75	50	600
			Pelletizer (kg/h)		
A.1 (C.5)	56	50	40	50	200
A.1 (C.6)	56	50	1000	50	200
A.1 (C.7)	56	50	1500	50	200

Table 3 shows all tests in Scenario 3 and how the parameters are changed during tests (highlighted in yellow). Below are short descriptions of the aspect of the system each group (A-E) aims to pinpoint

Group A: CHP Generation
Configurations A.2 and A.3 investigate the sizing of the CHP unit relative to the farm's base-load requirements. By scaling CHP electric capacity from 28 kW (50 % of baseline) to 112 kW (200 % of baseline), the model assesses how different straw pellet combustion rates affect the TES fill-level dynamics and the overall availability of power to the pelletizer, pyrolyzer, and climate control systems.

Group B: ORC Optimization
Configurations evaluate the ORC engine's role in "peak-shaving." By adjusting the ORC engine capacity from 25 kW to 75 kW, the study identifies the optimal rate at which stored thermal energy in the TES should be converted back into electricity to support BES recharging during nocturnal load spikes without limiting the system's CSR.

Group C: Fuel Quality
Group C represents the most granular sweep, ranging from 11 kW to 76.5 kW per 500 kg,h for the pelletization unit. This is designed to determine the effect of the pelletizer on the availability of energy to other components. The literature discussed in section 3.4 states that high-quality fuel poses fewer handling and safety risks, but requires more energy input. If the system can produce high-quality pellet fuel without depleting the BES or choking the energy system during peak loads, it would be of great value.

Group D: System Saturation
Configurations D.1 and D.2 focus on the pyrolyzer's ability to productively use excess energy to sequester carbon. While these changes may have a marginal effect on electrical self-sufficiency, they are critical for evaluating CSR capabilities without draining the TES and, in turn, the BES. This sweep determines how the pyrolyzer's capacity affects the system's overall energy performance and the carbon sequestering ratio.

Group E: PV Contribution
Configurations E assess the impact of solar generation scaling on the farm’s total energy balance. By varying the PV array size from 0 to 600 m^2, the model assesses how changes in direct solar electricity generation offset the need for CHP-derived power, thereby influencing the tractors' charging dynamics and altering the biomass boiler's seasonal fuel consumption rate.

Group A (C): Fuel Throughput
Group A (C) represents the pelletization unit's processing capacity. This is designed to find the effects of the BE fuel throughput. If Configuration A (C.5) results in system failure during the winter months despite raw straw being available, it indicates that the pelletizer’s processing speed is a logistical chokepoint preventing the CHP from operating at full capacity. This group also serves as a measure of how limited or excessive pellet processing affects the carbon-sequestering performance of components later in the system.

5 Results and Analysis

This chapter presents the results of the Simulink simulation and the data for each scenario and subgroup, along with accompanying analysis.

5.1 Scenario 1 (Baseline)

Table 4: Scenario 1, KPI results

Measure	***SSR (%)***	***BES,SoC<10 (%)***	***BES,SoC>95 (%)***	***TES,SoC<55 (%)***	***TES,SoC>95 (%)***	***R_C (kWh/kg)***	***Straw (Tonnes)***	***Biochar (Tonnes)***
Value	100	5,3	64,5	21,5	21,4	1,8	147.8	154,3

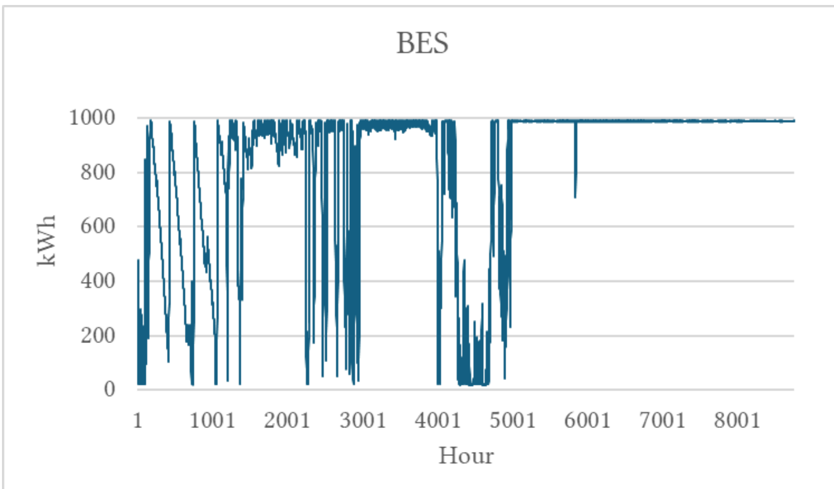

Figure 8: Scenario 1 BES SoC over a one-year period (2010)

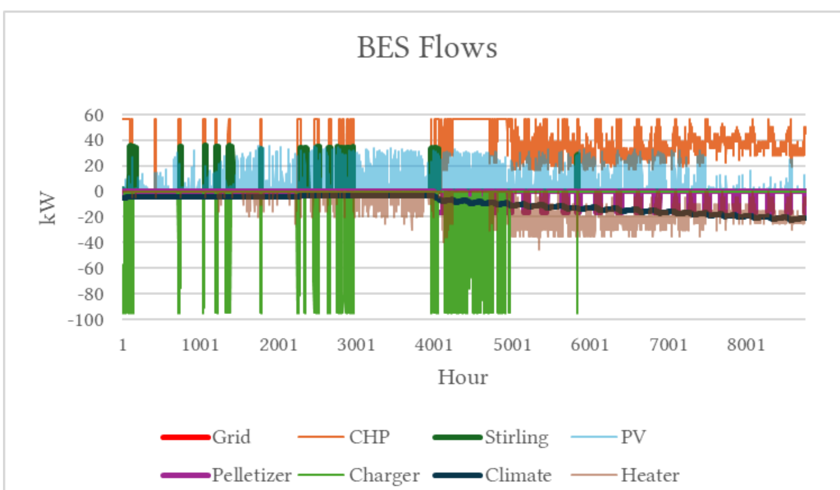

Figure 9: Scenario 1 BES energy flows over a one-year period (2010)

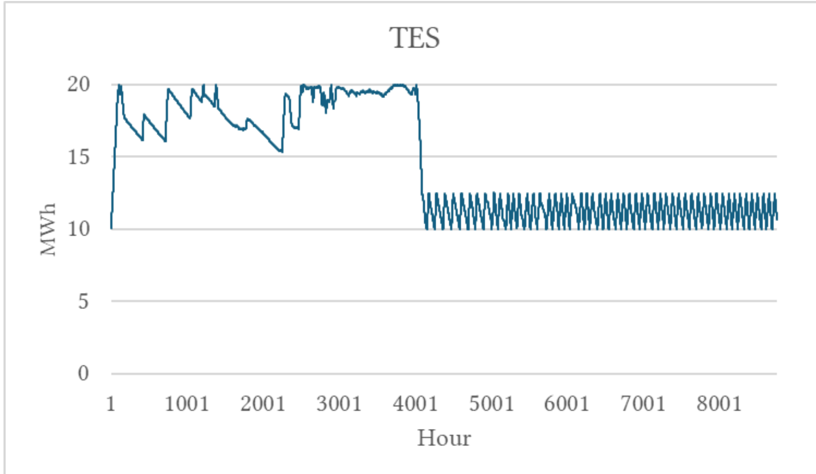

Figure 10: Scenario 1 TES SoC over a one-year period (2010)

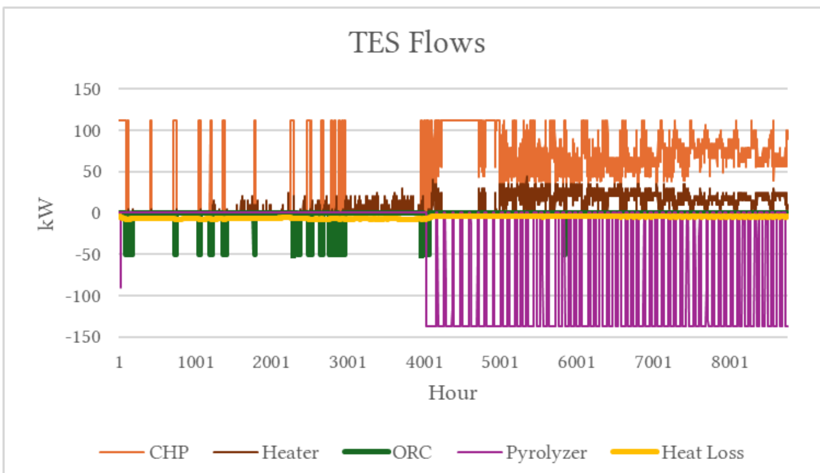

Figure 11: Scenario 1 TES energy flows over a one-year period (2010)

5.1.1 Scenario 1 Analysis

The primary objective of Scenario 1 was to determine whether a 200-hectare Swedish wheat farm could sustain its energy systems' electrical operations entirely off-grid using only locally sourced BE and PV generation. The simulation results demonstrate clear success: the baseline configuration (A.1) achieved 100 % SSR (See Table 4), exceeding the targeted 99 % threshold without requiring any energy from the national grid. This confirms the technical viability of the proposed energy loop under standard meteorological conditions for the Uppsala region.

The success of the 100 % SSR heavily relies on the system's Energy Control Logic, which prioritizes solar power. Because PV generation is highly seasonal in Sweden, the farm acts as a dual-mode system. During the summer months, the PV array serves as the primary energy source, reducing demand on biomass reserves, as seen between the 3000-4000 hour marks in figures 9 and 11. However, as solar irradiance drops in the autumn and winter, the system transitions to rely on the CHP generator. The simulation shows that the farm yields enough biomass during the early-fall harvest, about 4000-hour mark (See appendix 1, A.1), to supply the pelletizer, CHP, and pyrolyzer through the low-solar months and into the next year. Specifically, the farm ended the simulated year with a surplus of 147.8 tonnes of raw straw (See Appendix 1) out of the about 800 tonnes of wheat straw harvested, proving that the

200-hectare field produces far more BE than the system currently requires to operate. If the pyrolyzer, and with it the carbon sequestration function, are disabled the energy system would be able to supply the grid with power during peak load hours or alternatively the farmland allocated for energy could be significantly reduced. The harvest considered from the field is much larger than in the realistic case; the extreme case shows that, despite producing over 100 tonnes of biochar, the system remains stable and has energy to spare.

The robustness of this self-sufficient loop is further evidenced by the BES and TES SoC KPIs. Throughout the year, the BES maintained a SoC above 95 % for 64.50 % of the time, while also achieving a TES SoC >95 % for 21.5 % of the time. This indicates that for nearly two-thirds of the year, the system is in a generation surplus and the energy storages are often full. Furthermore, the BES dropped below the critical 10 % SoC threshold for only 5.30 % of the simulated year, which is noticeable but currently occurs only during a short period of simultaneous harvest, pelletization, and pyrolysis. This confirms that the electric generation capacity, specifically the ORC and CHP outputs, is appropriately sized to maintain system supply during extended periods of low solar yield or high fieldwork loads, thereby preventing localized blackouts.

However, the massive surplus of charge in the energy storages (64.5 % of the time >95 % BES.SoC, and 21.5 % of the time >95 % TES.SoC) hints that the baseline PV or CHP might actually be over-sized or that the energy system is missing opportunities to capture curtailed energy, energy that can be used for other agricultural purposes. While the baseline configuration demonstrates theoretical success, it is important to contextualize these findings within the limitations of the current modeling framework. Many of the farm's functions (food processing, drying of straw, farmers private electric consumption, et.c) have been subtracted and their electric and thermal load profiles would improve the accuracy of the model.

The robustness of 100 % SSR should be interpreted as an upper bound on performance potential rather than an absolute guarantee for real-world deployment. Because of this, the analysis should remain under certain scrutiny. The system exhibits clear signs of over-engineering. The finding that the BES maintains an SoC above 95 % for over 64 % of the year suggests that the current electric capacity is significantly larger than is required to maintain the 99 % SSR threshold. As shown in Figure 8, after the 5000-hour mark, the BES becomes saturated when the system is set to pyrolysis, as the CHP works overtime to deliver sufficient heat. Because the pyrolyzer depends on thermal input and both BES and TES are charged by the CHP during periods of high thermal demand, this might suggest that the energy delivered to the BES is not utilized effectively during pyrolysis.

From a techno-economic perspective, this represents an inefficient allocation of capital expenditure, suggesting the BES or CHP is far above the required dimension, or that alternative electric load-heavy systems (greenhouses, national grid supply, et.c.) should be implemented to curtail this surplus energy. Finally, future iterations should investigate at what point a reduction in battery size begins to impact reliability and the extent to which excess electrical energy can provide grid-supply services.

5.2 Scenario 2 (Non-TES)

Table 5: Scenario 2, KPI results

Measure	**SSR (%)**	**BES,SoC<10 (%)**	**BES,SoC>95 (%)**	**TES,SoC<55 (%)**	**TES,SoC>95 (%)**	**R_C (kWh/kg)**	**Straw (Tonnes)**	**Biochar (Tonnes)**
Value	56,5	48,1	21,6	-	-	3,9	26.9	164,1

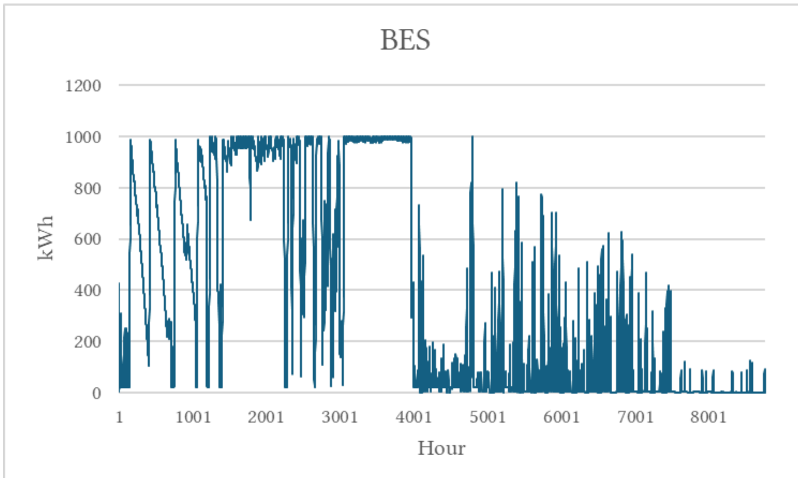

Figure 12: Scenario 2 BES SoC over a one-year period (2010)

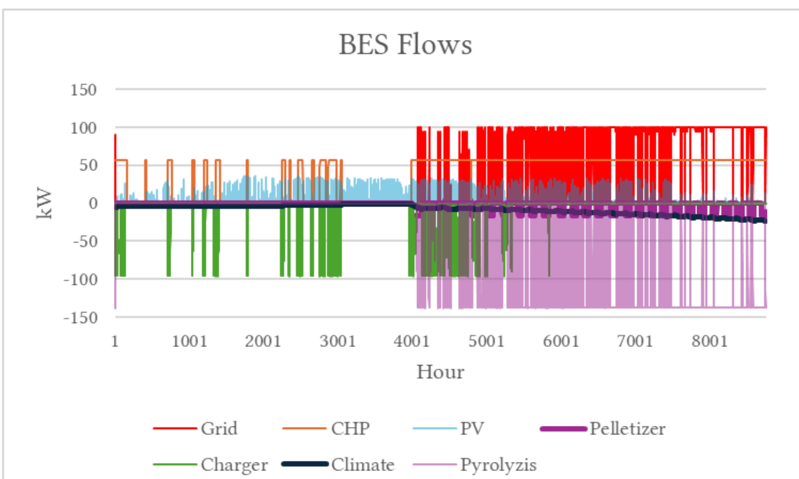

Figure 13: Scenario 2 BES energy flows over a one-year period (2010)

5.2.1 Scenario 2 Analysis

The comparative analysis of Scenario 2 isolates the technical and systemic impacts of TES by evaluating the farm's performance in the total absence of TES and with it the ORC function. The results reveal that the TES is not just an optimization component, but a fundamental requirement for the farm's self-sufficiency. When the 20 MWh TES is removed, the farm's ability to maintain electrical autonomy collapses, with the SSR falling from a perfect 100 % in the baseline to a critical 56.5 %. This 43.5 % energy coverage deficit indicates that, without a thermal buffer, the system is fundamentally incapable of meeting the electrical demands of autonomous tractors and farm operations year-round.

This failure of autonomy stems from a loss of the exergetic thermal energy produced by the CHP and stored in the TES for later utilization by the ORC engine. In the Baseline scenario, the TES acts as an energy reservoir, allowing the ORC to generate electricity during periods of low solar irradiation or high demand by drawing on stored heat. In Scenario 2, the absence of this buffer forces the system to use a significantly larger portion of BE simply to maintain operation and prevent blackout. Without the ability to store thermal energy generated during biomass combustion, the ORC cannot be dispatched to support the BES during peak loads or at night. Consequently, once the BES is exhausted, the farm has no secondary power stream to maintain the microgrid, leading to frequent and sustained power outages and enabling emergency grid support seen around the 5000-hour mark in Figure 12 as a sharp downturn in BES SoC and in Figure 13 as the flickering of red spikes from the grid-connection.

The lack of thermal buffering also leads to a significant reduction in resource efficiency. A paradoxical trend is observed: Scenario 2 consumes significantly more fuel than the baseline, even though it meets less than 60 % of the energy demand. Remaining straw reserves at the end of the year plummet from 147.2 tonnes in Scenario 1 to just 26.9 tonnes in Scenario 2 (See Appendix A.1 and A.2). This suggests that the CHP unit is forced to operate at lower total system efficiency, frequently running to meet instantaneous electrical loads while the concurrent heat production is wasted because it cannot be stored for later use. While this aggressive combustion strategy yields a slightly higher biochar of 164.1 tonnes compared to 154.3 tonnes in the baseline, this minor increase in byproduct, but near-depletion of the farm's annual biomass supply means that the CHP must be configured to use some of the biochar as fuel so not to risk total loss of energy security for the following year.
Furthermore, removing the TES places extreme stress on the electrical storage infrastructure. The BES spends 48,1 % of the year at an SoC below 10 %, a significant increase from the 5.3 % observed in the baseline. This chronic deep-discharge state is due to the heavy load the pyrolyser puts on the BES after the harvest around the 4000-hour and indicates a system under constant strain, which would likely accelerate battery degradation and increase long-term maintenance costs.

Ultimately, the results of Scenario 2 demonstrate that the TES serves as a much-needed energy reserve for the autonomous farm. By decoupling the timing of biomass combustion from that of electric energy demand and utilizing otherwise lost thermal energy, the TES transforms a failing, resource-depleting energy model into a robust, 100 % self-sufficient operation. These findings provide a definitive answer to research question 2, establishing that heat energy storage is essential for agricultural energy autonomy in a Swedish context under equal circumstances, even without many of the purely thermal-demanding farm processes included in the simulation.

5.3 Scenario 3 (Parametric Sweep)

Below, the reader finds the result of the parametric sweep for each group in scenario 3 compared to each other columnwise in colorcode; Green value indicates a comparatively good value, yellow a median, and red a poor value. For example: In column 3 "BES,SoC < 10 (%)", A.3 indicates an exceptional performance with barely any annual hours where the BES is depleted, compared to C.4 within the same column that shows significant time with low BES charge.
The "SSR (%)" column displays only a binary color code of green (Passed SSR threshold) and red (Did not pass SSR threshold).
The "Straw (Tonnes)" column is not color coded as

Table 6: Scenario 3, KPI results (Comparison)

Config.	SSR (%)	BES,SoC<10 (%)	BES,SoC>95 (%)	TES,SoC<55 (%)	TES,SoC>95 (%)	R_C (kWh/kg)	Straw (Tonnes)	Biochar (Tonnes)
A.1	100	5.3	64.5	21.5	21.4	1.8	147.8	154.3
A.2	100	16.1	55.5	21.5	7.2	2.1	385.2	95.9
A.3	100	0.1	62.7	16.1	19.7	1.7	0	193.4
B.1	100	7.3	62.7	21.6	14.7	1.8	147.2	154.9
B.2	100	5.2	64.2	21.5	16.3	1.8	137.5	154.5
C.1	100	5.4	64.6	21.9	11.8	1.8	149.2	155.0
C.2	100	5.7	63.1	21.9	21.7	1.8	116.7	156.7
C.3	100	6.2	63.8	21.4	23.1	1.8	125.2	157.4
C.4	97.2	17.1	45.3	21.9	23.2	2.8	80.8	165.2
D.1	100	4.9	60.9	0.1	23.4	2.1	288.0	118.3
D.2	100	6.2	63.9	21.7	23.0	1.8	140.3	155.6
E.1	100	9.2	47.0	21.0	12.6	1.6	134.8	151.0
E.2	100	2.0	71.1	21.4	17.7	2.1	165.8	152.1
E.3	100	1.5	75.0	21.2	30.0	2.3	176.2	151.5
A.1 (C.5)	100	2.9	40.3	0.1	15.8	4.6	629.0	38.5
A.1 (C.6)	100	4.6	64.8	21.4	22.8	1.8	138.7	152.8
A.1 (C.7)	99.9	5.0	62.3	21.8	21.3	1.8	148.8	150.9

5.3.1 Scenario 3 Analysis

Group A

By reducing the CHP capacity in A.2 by 50 %, the results show that the percentage of time the BES dropped below the critical 10 % SoC threshold for A.2 increased to 16.10 %, compared to 5.30 % in the baseline. This indicates that a smaller CHP unit is less able to recover battery charge during periods of low solar input and high demand, forcing the system to operate much closer to its operational limits. While the TES remained above the 55 % SoC threshold, as with A1, it performed the worst of all groups in terms of TES saturation, with SoC above 95 % for only 7.2 % of the year. Additionally, biochar production fell to 95.9 tonnes, a 37.8 % decrease from the baseline's 154.3 tonnes. This reduction highlights a critical trade-off: when energy production is throttled, the system prioritizes basic electrical loads over the high-thermal-demand pyrolysis process. Doubling the CHP capacity in A.3 significantly improved energy storage stability, with the BES dropping below 10 % SoC for only 0.10 % of the year and the TES below 55 % SoC for 16.1 % less time discharged compared to baseline (21.9 %). This oversizing allows the system to rapidly recover both BES and TES reserves, as evidenced by an increase in biochar production to 193.4 tonnes, and the availability of thermal energy specifically enables the main energy sink, pyrolysis, to operate more frequently. The A.3 test also showed the best R_c value, presumably due to the high biochar yield resulting from excess available energy.

However, the increased combustion rate necessitates careful monitoring of the TES. While the system remained stable, the higher throughput suggests that oversizing the CHP must be balanced with the thermal storage capacity or increasing thermal sinks to avoid exceeding the TES limit. The deduction of group A is that an increased capacity for thermal output improves the overall carbon sequestering functions of the system, and that the PV and ORC engine balances the energy distribution sufficiently to meet the SSR requirement even at decreased CHP capacity.

Group B

The parametric sweep for Group B examined the impact of adjusting the ORC engine capacity to determine its effectiveness in peak-shaving, the conversion of stored thermal energy into electricity during periods of high electrical demand or low renewable generation. The analysis indicates that ORC engine capacity is not a primary driver of system failure or systemic stress within the tested range, as both B.1 and B.2 configurations maintained 100 % SSR, confirming that the baseline ORC capacity is appropriately sized to manage the farm's base electrical load fluctuations. KPI showed minimal deviation from the A.1 baseline; specifically, in configuration B.1, the time the BES dropped below the 10 % SoC threshold increased slightly to 7.30 % compared to 5.30 % in the A.1 baseline, while configuration B.2 improved BES stability, with the time below 10 % SoC dropping marginally to 5.20 %.

These results suggest that while an increased ORC capacity provides a marginal improvement in battery health by more effectively converting thermal reserves into electricity, the system's sensitivity to ORC size is relatively low.

Furthermore, thermal dynamics remained stable, with TES saturation levels (SoC > 95 %) showing negligible difference across B.1 and B.2, and biochar production remaining remarkably consistent at approximately 154.5 tonnes, nearly identical to the baseline’s 154.3 tonnes. Consequently, the ORC engine provides a flexible buffer for electrical generation without compromising the system's SSR or thermal storage integrity. Because the current baseline configuration is already highly optimized, ORC capacity does not represent a critical bottleneck in the system.

Group C
The results demonstrate that the system is highly sensitive to the energy efficiency of the pelletization process. Configurations C.1 through C.3 maintained a 100 % SSR, with KPI values closely aligned with the A.1 baseline. Specifically, these configurations successfully supported the farm's load while keeping battery stress manageable, as evidenced by the percentage of time the BES remained below the 10 % SoC threshold, which changed only slightly from 5.30 % to 6.20 %. In these cases, the energy penalty associated with pelletizing was sufficiently low to allow the CHP system to effectively recover BES levels. However, the decrease in electric load resulted in a noticeable depletion of the TES, with SoC falling below 55 %, an increase of 21.9 % compared to 21.7 % (baseline), a seemingly small change but noticeable, as the lower threshold requires severe thermal depletion to be breached. The CHP was less frequently active, and this was particularly evident for C.1, where TES SoC > 95 % was only 11.8 % compared to a baseline of 21.4 %, indicating that low electric load for fuel processing saturated the BES while choking the TES.

When the pelletizer energy requirement was increased to 76.5 kWh/kg in C.4, the system failed to maintain the target autonomy, with the SSR dropping to 97.2 %. This performance decline was accompanied by a marked increase in systemic stress, as the BES SoC dropped below the 10 % threshold for 17.10 % of the year, a significant increase compared to the 5.30 % observed in the baseline. Furthermore, the percentage of time the BES remained above 95 % SoC fell to 45.3 %, while the percentage of time the TES SoC fell below increased to 21.9 %, indicating that the high energy demand of an inefficient pelletizer severely limits the system's ability to store excess energy.

In conclusion, the pelletization unit represents one of the more sensitive bottlenecks identified in the energy system. While the farm can absorb moderate variations in fuel-processing efficiency, the analysis confirms that energy-inefficient pelletization (C.4) rapidly depletes the system's energy reserves, undermining electrical autonomy but not carbon sequestration, whereas extreme electrical efficiency chokes the TES. These findings underscore the need to balance industrial-scale production with high-quality, efficient pelletization.

Group D
The simulation results reveal a distinct relation between biochar production and energy capacity. In configuration D.1, where pyrolyzer utilization is minimized, the TES SoC drops below 55 % only 0.10 % of the time, reflecting a high degree of thermal excess. However, this conservative approach limits biochar production to 118.3 tonnes. Increasing the pyrolyzer capacity in configuration D.2 produced 155.6 tonnes of biochar, which is comparable to A.1. This increase is accompanied by a marginal difference in the system's thermal buffer: the TES SoC drops below the 55 % threshold to 21.70 %, indicating similar thermal stability to the A.1 configuration, with some stress applied. This stress is also noted as BES SoC <10 % increase to 9.2 %.

These findings indicate that while the pyrolyzer effectively utilizes surplus energy that would otherwise be curtailed, its operation is tied to the system's thermal availability. Because the pyrolyzer consumes energy that is also required to support the ORC engine, over-sizing its capacity risks depleting the thermal reserves necessary for low-solar electrical production. The optimal configuration for a sustainable farm operation requires a balanced pyrolyzer capacity that maximizes biochar sequestration while maintaining sufficient thermal head in the TES to ensure continuous BES support through the ORC and overall electrical self-sufficiency. Alternatively, an increase in pyrolysis capacity must be accompanied by an increase in CHP capacity to avoid thermal depletion. This would improve carbon sequestering capabilities, but might oversaturate the BES without a proportionally appropriate electrical sink.

Group E

This segment of the parametric sweep examined the influence of PV generation capacity on system autonomy, specifically how variations in solar input affect the balance between the BES and the TES. Configurations E.1 (no PV) and E.2-3 (expanded PV) were tested against the baseline to determine the PV system's role as both a primary electrical source and a strategic secondary generator. The analysis reveals that PV generation is a critical lever for protecting battery health, although its contribution to overall system stability is highly seasonal.

In configuration E.1, where PV generation was removed, the system exhibited significantly increased stress on the BES; the percentage of time the battery dropped below the 10 % SoC threshold increased to 9.20 %, compared to 5.30 % in the baseline. This demonstrates that when solar contribution is limited, the CHP and ORC must compensate for the deficit, effectively forcing the system to operate at higher electrical load levels and reducing the safety margins for battery endurance. Configuration E.3, which drastically scaled up PV capacity, improved BES stability, with the time below 10 % SoC falling to just 1.50 %.

However, this high level of solar integration introduced a new challenge regarding thermal management. The TES experienced significant saturation, remaining above 95 % SoC for 30.00 % of the year. This indicates that while solar energy effectively displaces the need for CHP-derived electricity, the lack of a sufficient thermal sink for the excess energy, coupled with the heat retained from the now-underutilized CHP unit, leads to thermal storage or sink bottlenecks.

Group A (C)

The final tests focus on the pelletization process capacity to identify how the lack of BE fuel affects system performance. C.5 limited straw processing to match the fuel consumption of the CHP and show surprisingly stable results as the lower threshold for both BES and TES are rarely breached with 2.9 % and 0.1 % respectively compared to the 5.3 % and 21.5 % in the baseline. Unfortunately, the lack of available BE prevents both BES and TES from reaching upper saturation levels, as reflected in the low system biochar output of only 38.5 tonnes and the high R_C. This indicates that restricted throughput creates a major bottleneck for the pyrolyzer. Low fuel processing still provides enough energy to meet the SSR requirements, but this is not the case for C.7, with an SSR of 99.9 %. The probable cause is the increased electrical load from the oversized pelletizer, combined with other electrical sinks, which occasionally depletes the BES and forces the emergency grid connection. Despite the increased availability of pellets, biochar production remains limited to a level comparable to baseline, indicating that pellet availability must be accompanied by increased CHP capacity to enable efficient pyrolysis.

7 Discussion

7.1 Self-sufficiency

The simulation of the baseline configuration (Scenario 1) demonstrates that achieving a 100 % SSR for a 200-hectare Swedish wheat farm is technically feasible using a combination of PV, biomass-fired CHP, and dual-mode energy storage. By strictly defining the system boundary to exclude any continuous support from the national grid, the model proved that the internal energy loop can sustain all operations, including the high-demand fieldwork of autonomous electric tractors and pyrolysis, without breaching the 99 % success threshold.

Unfortunately, this technical success must be reconciled with the practical and economic realities of the infrastructure required to sustain such autonomy. The backbone of this 100 % SSR is the massive energy storage infrastructure of the 1 MWh BES and a 20 MWh TES. For a single 200-hectare farm, a 1 MWh battery array represents a significant capital investment that exceeds typical contemporary agricultural installations and practicality of maintaining a 20 MWh molten salt tank, as described in section 4.3.5, poses substantial engineering, financial and safety challenges for an individual farmer. The necessity of this infrastructure is underscored by Scenario 2, which showed that removing the TES causes the SSR to collapse to 56.5 %. This suggests that while 100 % autonomy is possible, it is made possible entirely by a large exergetic thermal buffer that decouples heat production from immediate electricity demand.
Furthermore, the pursuit of a perfect 100 % SSR versus the targeted 99 % margin highlights the law of diminishing returns in off-grid energy systems. The baseline model achieved 100 % SSR, but the results from Groups A and C in the parametric sweep show how easily this autonomy can be compromised.

For example: When the pelletizer's energy requirement was increased to 76.5 kWh/t (test C.4), the SSR dropped to 97.2 %, and systemic stress on the BES increased significantly. This drop in autonomy represents a critical failure in a purely off-grid system, as it implies a total blackout or the inability to complete fieldwork during key seasonal windows. In a real-world application, the cost and complexity of scaling the BES and TES to cover the final 1-3 % of energy demand may far outweigh the benefits of total grid independence. A hybrid approach in which the farm remains grid-connected to handle rare peak-load failures while maintaining a 95-98 % SSR would likely provide a more resilient and economically viable path to the transition to fossil-free agriculture.

Despite this, the most significant finding regarding the system's architecture is the necessity of the TES unit. While the TES is often viewed as a secondary component in modern microgrids, the results of Scenario 2 reveal that the system's autonomy requires capturing the thermal energy produced by the CHP boiler. Without a TES, the SSR plummeted from 100 % to 56.5 %. This drop of nearly 44 percentage points suggests that the BES alone, even at a large 1 MWh capacity, is insufficient to manage the temporal misalignment between energy production and the high-intensity demands of autonomous electric tractors and pyrolysis. The role of the TES in this configuration is best understood as an exergetic buffer that decouples the thermal energy supply from the electrical demand.

In the baseline model, the ORC engine serves as a secondary link between the biomass furnace and the farm's electrical grid. By using the TES to store high-temperature heat, the system allows the ORC engine to respond to electrical load requirements rather than being tethered to the biomass boiler's instantaneous output. This decoupling is critical during peak operational windows, such as harvest or sowing, when the electric tractors impose heavy, concentrated loads on the system. Without the TES, the ORC engine can only provide power when the furnace is actively firing; any surplus thermal energy is essentially wasted, and any deficit must be met by the BES, which quickly reaches its lower SoC threshold under such strain.

Furthermore, the TES provides a level of system resilience that is more cost-effective than scaling the BES to comparable energy densities. Storing 20 MWh of thermal energy in a battery array would be economically and chemically prohibitive for a farm of this scale, but the exact size and configuration of the TES require further investigation to find a feasible design for a farmer. By storing energy as heat, the system exploits the lower per-kWh cost of thermal storage media to provide long-duration energy balancing. This synergy allows the BES to function as a "high-speed" buffer for immediate voltage stability and short-term tractor charging peaks, while the TES handles the "heavy lifting" of shifted energy loads over several days or weeks. The collapse of the SSR in Scenario 2 proves that for a biomass-integrated farm, the energy system’s backbone is thermal, and the ability to manage heat is what ultimately determines the ability to provide reliable power.

7.2 Bottlenecks

The parametric sensitivity analysis conducted in Chapter 6 highlights that while the system is robust under baseline conditions, its autonomy is sensitive to specific technical efficiencies and sizing choices. The most prominent bottleneck identified is the energy intensity and capacity of the pelletization process. As noted in the literature review, there is a significant discrepancy between lab-scale pelletizers (consuming up to 153 kWh/t) and optimized commercial units (22–60 kWh/t). The results from Scenario Group C demonstrate that the farm’s 100 % SSR is highly vulnerable to this variable. When the pelletizer demand was increased to 153 kWh/t (test C.4), the SSR fell to 97.2 %. This identifies pelletization not just as a processing step, but as a potential "energy drain" that can destabilize the entire microgrid if not managed with high-efficiency equipment. For a farm aiming for total autonomy, investing in industrial-grade, low-energy pelletization of appropriate capacity is not merely an economic choice but a technical requirement for system stability.

A second critical bottleneck is the sizing of the CHP unit relative to fluctuating thermal loads, battery charging requirements, and pyrolysis capacity. The results from test group A reveal a non-linear relationship between CHP capacity and system performance.

Reducing the CHP size to 50 % of the baseline did more than just reduce energy output and forced the system to prioritize essential electrical loads, specifically tractor charging, at the expense of biochar production. The 37.8 % reduction in biochar yield in test A.2 occurs because the surplus thermal energy required for the pyrolysis process is the first resource to be sacrificed when the CHP cannot meet the simultaneous demands of the ORC engine and the electric heavy loads.

These findings suggest that "the bottlenecks in an autonomous farm system are a multi-layered issue. To maintain 100 % SSR, the system must be sized not for average conditions but for worst-case scenarios. Energy output and inputs must be temporarily matched while also providing a practical, economically feasible system. The CSR's sensitivity to these energy bottlenecks further implies that the farm's role as a carbon sink is intrinsically linked to its energy surplus, suggesting that, once the energy margin disappears, the environmental benefits of biochar production are the first to be lost. If the priority is to maintain 100 % self-sufficiency, the system could adjust biochar production. In reality, the need for biochar for the fields and power to the farm, or potentially the grid, would differ from year to year, and the system would have to be properly designed for the functions it needs to perform within realistically larger borders than the one in this thesis.

7.3 Implications of the Delimitations

The case study omits many aspects of objective reality, largely due to the author's limited time for this thesis. Similar to the previous segment, this one will go through the system from the wheat field to biochar, listing some of the major limitations needed to keep the scope within reasonable bounds.

While the simulation provides a technical proof of concept for farm autonomy, several deliberate simplifications and delimitations must be acknowledged to contextualize the findings. The primary delimitation concerns the physical and economic boundaries of the storage systems. In the model, the storage capacities for raw biomass (straw/pellets) and the byproduct (biochar) were set to unlimited to allow the system to operate without physical-volume constraints. In a real-world application on a 200-hectare farm, the logistics of storing hundreds of tonnes of straw would require significant barn space and fire-safety infrastructure. Similarly, the accumulation of biochar over a full year represents a substantial volume that must be integrated into the farm's soil management cycle or transported off-site, neither of which was accounted for in the system's energy or labor balance.

Probably the most significant theoretical simplification in the model lies in the thermodynamic representation of the biomass-to-electricity and thermal-to-electricity conversion processes. The thesis models CHP- and ORC-based electricity generation as linear and instantaneous, ignoring the physical reality of boilers, which have startup periods and require stable combustion conditions to operate properly. This binary approach to modeling the CHP, ORC, and the pyrolyzer creates a huge discrepancy between the model and reality, and had to be adopted to simplify an already huge project. What this does is condense a system that would be efficient and dynamic under ideal conditions and try to describe it in low resolution.

The oversizing of the BES and TES was due to the rapid fluctuations these binary gains/sinks created, and lower energy storage capacities meant that the BES and TES saturated and depleted almost instantaneously. A dynamic system could operate more smoothly within tighter margins and adjust components more accurately, and predictive computing could meet power requirements in slow systems long before they are needed.

Similarly, the ORC engine is modeled on the temperature differential between the storage medium and the ambient environment described by equation 3 in section 3.8. This idealized approach, which notably conflates ORC mechanics, relies on a simplified efficiency equation that mirrors theoretical maximums rather than operational realities. Real-world ORC cycles are subject to mechanical friction, parasitic pump work, and heat exchanger limitations. More importantly, these engines suffer severe efficiency degradation at part load.

By assuming a linear power-conversion rate, the simulation likely overestimates the usable electricity recovered from the TES, particularly during rapid load-following periods required to stabilize the BES.

Likewise, the pyrolysis process is modeled with a high degree of simplification that heavily influences the system's energy balance. In the Simulink model, pyrolysis is approximated as a static energy sink that requires a constant rate of mass and energy and instantaneously switches between states. This deliberate delimitation excludes the thermodynamic complexity of slow pyrolysis, particularly the generation and potential utilization of syngas and bio-oil byproducts. In commercial applications, the syngas produced is often recycled to fuel the thermal reaction, thereby making the process quasi-autothermal and drastically reducing external energy inputs. By ignoring the syngas energy loop, the model assumes the worst-case energy cost for biochar production. Conversely, the system logic treats the pyrolyzer as a highly flexible component that can serve as an instant thermal sink for excess energy. This overlooks the physical reality of thermochemical reactors, which require prolonged ramp-up periods, stable high-temperature environments, and gradual cool-downs, making them poorly suited for rapid, intermittent peak-shaving operations.

In the current Simulink model, these components are governed by state-dependent control loops that switch them directly from zero to full nominal capacity the moment specific SoC thresholds are breached. This binary operation ignores the inherent thermal inertia of biomass combustion and thermochemical reactors. By assuming instantaneous state changes, the simulation essentially treats heavy thermal machinery with the same rapid agility as a solid-state battery inverter. This likely underestimates the parasitic energy and fuel costs of warming up the equipment, while overestimating the system's ability to seamlessly follow highly erratic electrical loads. A more accurate evaluation of the system would require implementing dynamic operational functions into the model, such as defined thermal ramp rates, part-load efficiency curves, standby modes, and minimum run-time constraints. Integrating these thermodynamic transients would provide a much more realistic assessment of the system's true responsiveness, potentially revealing that the BES must endure longer interim load strains while the thermal components slowly come online.

Another critical technical limitation of the model is the inability to account for BES degradation. The simulation treats the 1 MWh lithium-ion battery array as a static component with a constant capacity. In reality, these batteries undergo cyclic aging and capacity degradation. Given that the farm's autonomy relies heavily on the BES to buffer the high-intensity loads of the electric tractors, any reduction in capacity would eventually cause the SSR to drift below the 99 % success threshold. Therefore, the 100 % SSR achieved in the baseline model should be viewed as a "Day One" performance metric. For long-term planning, the BES would likely need to be oversized by 20-25 % at the time of installation or factored in as a major capital replacement halfway through the system's lifecycle.

Notably, the amount of wheat straw harvested is constant across a 200 ha field. Realistically, both the area and the weather conditions of the year would vary, and with them, the amount of straw harvested. Much like the binary nature of the CHP and pyrolyzer, this part of the project was simplified. The real system would plan the output of the fields to match the needs of the energy system, as well as the agricultural businesses operating on the rest of the farmland. Most likely, "power-crops" could be added to the list of farms with rotational crops, and growing your own power becomes a part of green agriculture, much like salix is grown to burn in power plants.

Reliance on a single year and location of Swedish weather data (Solar and Temperature) introduces some stochastic risk. While the chosen dataset represents a typical meteorological year, it does not account for worst-case climate scenarios, such as a succession of exceptionally cloudy summers or abnormally cold winters, which would increase the domestic thermal load while decreasing PV yield. The control logic within the Simulink model operates with "perfect information" regarding current states, whereas real-world sensors and automated control systems must deal with latency, calibration errors, and mechanical wear. While these limitations do not invalidate the findings, they suggest that the theoretical autonomy demonstrated here provides an idealized benchmark that real-world implementations would strive to approach through conservative engineering and redundant system design.

7.3 Opportunities

The baseline results indicate that while the system is designed to ensure 100 % autonomy during peak agricultural windows, it inevitably generates a significant energy surplus during periods of tractor inactivity and peak summer months. In a standard microgrid, this excess electricity would be curtailed and excess heat dissipated via cooling towers. On a Swedish farm, this surplus presents a strategic opportunity to diversify production by integrating high-intensity greenhouse systems. By utilizing low-grade waste heat from the ORC engine's cooling circuit and the pyrolyzer's exhaust, the farm can maintain a controlled environment for year-round vegetable or berry production, effectively transforming energy waste into a high-value food output. And the positive effects of the modeled energy system on greenhouse infrastructure are threefold: thermal, electrical, and chemical. Thermally, the TES can act as a buffer for both the CHP system and a hydronic greenhouse heating network. This allows for the cultivation of crops that would otherwise be climatically impossible in Sweden during winter, such as tomatoes or leafy greens. Electrically, the surplus PV yield in the summer, which often exceeds the BES's charging capacity, can be diverted to supplemental greenhouse lighting or automated climate control systems. This demand management approach uses the greenhouse as a flexible load to absorb energy spikes, thereby reducing the mechanical and chemical strain on system components. The integration of greenhouses also offers a pathway for chemical circularity through CO_2 fertilization and biochar application. The flue gases from the biomass-fired furnace, if properly scrubbed of particulates and NOx, can be enriched with CO_2 and injected into the greenhouse atmosphere to accelerate plant photosynthesis. The biochar produced can be used as a high-performance growing substrate within the greenhouse, improving nutrient retention and reducing the need for synthetic fertilizers. By transitioning from a linear model to a circular hub, the farm maximizes its exergetic efficiency and significantly improves its economic resilience, as surplus energy is used internally to generate a secondary revenue stream.

8 Conclusions

This chapter answers the research questions

1. Can a Swedish wheat farm be self-sufficient in electricity, utilizing only photovoltaics and locally sourced biomass?

Yes. The simulation results demonstrate that a 100 % SSR is technically achievable. By utilizing a PV and a biomass-fired CHP system integrated with both battery and thermal storage, the farm can meet all its electrical and thermal demands internally. This configuration successfully powers high-intensity operations, such as fieldwork with autonomous electric tractors and pyrolysis, while maintaining complete independence from the national grid.

2. Does heat energy storage improve the energy self-sufficiency of the farm, and to what extent compared to one without it?

Yes, TES is the fundamental backbone of the system's autonomy. The inclusion of a 20 MWh TES enables decoupling of heat production from electricity demand, providing a critical exergetic buffer. Without the TES, the farm's SSR collapses from 100 % to 56.5 %. This drop confirms that thermal storage is critical for stabilizing a biomass-integrated agricultural microgrid.

3. Which components can cause bottlenecks within the energy system, and can they be reasonably adjusted to address these issues?

The primary bottlenecks are the pelletizer's energy intensity and the CHP unit's nominal capacity. High-demand pelletizers can destabilize the system, dropping the SSR to 97.2 %, while an undersized CHP unit forces the system to prioritize essential operations and limit biochar generation. These bottlenecks can be reasonably adjusted by prioritizing the installation of high-efficiency, industrial-grade pelletizing equipment and sizing the CHP unit to meet peak concurrent loads rather than average annual demand. Additionally, oversizing the BES by 20-25 % is recommended to mitigate the long-term bottleneck of battery capacity degradation.

4. What and how much byproducts are produced, and how can they be utilized to perform environmental services?

Most scenarios produced over 100 tonnes of biochar that can be used for GHG sequestration and to improve soil nutrient and water retention. Hundreds of tonnes of harvested straw, both processed and unprocessed, can act as a renewable energy supply. Excess energy can also be utilized for complementary farm operations (Greenhouses, Aquaponics, Water treatment).

9 Future studies

The findings of this thesis establish a technical foundation for autonomous agricultural energy systems, yet several avenues remain for deeper investigation to bridge the gap between simulation and real-world deployment. Future research should prioritize a comprehensive economic and life cycle assessment (LCA). While this study proved technical feasibility, the capital expenditure required for a 1 MWh BES and a 20 MWh TES unit is substantial. An economic optimization study using levelized cost of energy (LCOE) or net present value (NPV) analysis would help determine the financial viability of such systems compared to grid-connected alternatives, particularly when considering the potential revenue from carbon credits generated by biochar sequestration. A critical technical evolution would involve the transition from steady-state logic to dynamic modeling. As discussed in the limitations, incorporating thermal ramp rates, part-load efficiency curves, and start-up energy penalties for the CHP, ORC engine, and pyrolysis unit would provide a more granular understanding of system stability. Future models could utilize predictive analysis of electric and thermal loads, optimizing the discharge cycles of the TES and BES to minimize wear while better meeting demands. And integrating BES and TES degradation models is essential to evaluate the system's performance over a 15- to 20-year horizon, ensuring that the 100 % SSR remains robust as hardware ages.

The baseline results indicate that, while the system is designed to ensure 100 % autonomy during peak agricultural windows, it inevitably generates a significant energy surplus during tractor inactivity and peak summer months. In a standard microgrid, this excess electricity would be curtailed and excess heat dissipated via cooling towers. On a Swedish farm, this surplus presents a strategic opportunity to diversify production by integrating high-intensity greenhouse systems. By utilizing low-grade waste heat from the ORC engine's cooling circuit and the pyrolyzer's exhaust, the farm can maintain a controlled environment for year-round vegetable or berry production, effectively transforming energy waste into a high-value food output. And the positive effects of the modeled energy system on greenhouse infrastructure are threefold: thermal, electrical, and chemical. Thermally, the TES can act as a buffer for both the CHP system and a hydronic greenhouse heating network. This allows for the cultivation of crops that would otherwise be climatically impossible in Sweden during winter, such as tomatoes or leafy greens. Electrically, the surplus PV yield in the summer, which often exceeds the BES's charging capacity, can be diverted to supplemental greenhouse lighting or automated climate control systems. This demand management approach uses the greenhouse as a flexible load to absorb energy spikes, thereby reducing the mechanical and chemical strain on system components. The integration of greenhouses also offers a pathway for chemical circularity through CO_2 fertilization and biochar application. The flue gases from the biomass-fired furnace, if properly scrubbed of particulates and NOx, can be enriched with CO_2 and injected into the greenhouse atmosphere to accelerate plant photosynthesis.

The biochar produced can be used as a high-performance growing substrate within the greenhouse, improving nutrient retention and reducing the need for synthetic fertilizers. By transitioning from a linear model to a circular hub, the farm maximizes its exergetic efficiency and significantly improves its economic resilience, as surplus energy is used internally to generate a secondary revenue stream.

References

1. Mellgren T. Agricultural sector [Internet]. Stockholm: Fossilfritt Sverige; 2026 Feb [cited 2026 Mar 12]. Available from: https://fossilfrittsverige.se/en/roadmap/the-agricultural-sector/

2. Naturvårdsverket. Arbetsmaskiner, utsläpp av växthusgaser [Internet]. Stockholm: Naturvårdsverket; 2025 Dec [cited 2026 Apr 8]. Available from: https://www.naturvardsverket.se/data-och-statistik/klimat/vaxthusgaser-utslapp-fran-arbetsmaskiner/

3. Regeringskansliet. Vägen mot fossiloberoende jordbruk [Report]. Stockholm: Regeringskansliet; 2021. 413 p
.
4. Judijanto L. Price Dynamics of Renewable Diesel HVO (UCO) in Europe: A Review of Supply, Demand, and Policy Determinants. Eur J Manag Econ Bus. 2026 Feb 19;3(2):49–73. doi:10.59324/ejmeb.2026.3(2).04

5. Kovačević Z, Bischof S, Bilandžija N, Krička T. Conversion of Waste Agricultural Biomass from Straw into Useful Bioproducts—Wheat Fibers and Biofuels. Sustainability. 2024 Jun 2;16(11):4739. doi:10.3390/su16114739

6. Agu OS, Tabil LG, Mupondwa E, Emadi B. Torrefaction and Pelleting of Wheat and Barley Straw for Biofuel and Energy Applications. Front Energy Res. 2021 Sep 28;9:699657. doi:10.3389/fenrg.2021.699657

7. El-Sayed SA, Elsaid Mohamed MK. Mechanical properties and characteristics of wheat straw and pellets. Energy Environ. 2018 Nov;29(7):1224–46. doi:10.1177/0958305X18772414

8. Whittaker C, Shield I. Factors affecting wood, energy grass and straw pellet durability – A review. Renew Sustain Energy Rev. 2017 May;71:1–11. doi:10.1016/j.rser.2016.12.119

9. Stelte W, Clemons C, Holm JK, Ahrenfeldt J, Henriksen UB, Sanadi AR. Fuel Pellets from Wheat Straw: The Effect of Lignin Glass Transition and Surface Waxes on Pelletizing Properties. BioEnergy Res. 2012 Jun;5(2):450–8. doi:10.1007/s12155-011-9169-8

10. Jones JM, Darvell LI, Bridgeman TG, Pourkashanian M, Williams A. An investigation of the thermal and catalytic behaviour of potassium in biomass combustion. Proc Combust Inst. 2007 Jan;31(2):1955–63. doi:10.1016/j.proci.2006.07.093

11. Chataut G, Bhatta B, Joshi D, Subedi K, Kafle K. Greenhouse gases emission from agricultural soil: A review. J Agric Food Res. 2023 Mar;11:100533. doi:10.1016/j.jafr.2023.100533

12. Javanmard A, Zuki FM, Patah MFA, Wan Daud WMA. Transforming biowaste to bioenergy: The role of catalysts in advancing thermochemical torrefaction. Process Saf Environ Prot. 2025 Apr;196:106779. doi:10.1016/j.psep.2025.106779

13. Guo W. Self-heating and spontaneous combustion of wood pellets during storage [Dissertation]. Vancouver: University of British Columbia; 2013. doi:10.14288/1.0073583

14. Butler JW, Skrivan W, Lotfi S. Identification of Optimal Binders for Torrefied Biomass Pellets. Energies. 2023 Apr 12;16(8):3390. doi:10.3390/en16083390

15. Björnsson L, Prade T. Sustainable Cereal Straw Management: Use as Feedstock for Emerging Biobased Industries or Cropland Soil Incorporation? Waste Biomass Valorization. 2021 Oct;12(10):5649–63. doi:10.1007/s12649-021-01419-9

16. North Dakota State University. Feeding Straw [Internet]. Fargo: North Dakota State University; [cited 2026 Apr 7]. Available from: https://www.ndsu.edu/agriculture/ag-hub/ag-topics/livestock/beef/nutrition-and-feeding/feeding-straw

17. Sarbu I, Sebarchievici C. A Comprehensive Review of Thermal Energy Storage. Sustainability. 2018 Jan 14;10(1):191. doi:10.3390/su10010191

18. Zhou D, Zhao CY, Tian Y. Review on thermal energy storage with phase change materials (PCMs) in building applications. Appl Energy. 2012 Apr;92:593–605. doi:10.1016/j.apenergy.2011.08.025

19. Cot-Gores J, Castell A, Cabeza LF. Thermochemical energy storage and conversion: A-state-of-the-art review of the experimental research under practical conditions. Renew Sustain Energy Rev. 2012 Sep;16(7):5207–24. doi:10.1016/j.rser.2012.04.007

20. Macchi E, Astolfi M, editors. Organic Rankine Cycle (ORC) Power Systems [Internet]. Duxford: Woodhead Publishing; 2017 [cited 2026 Apr 26]. Available from: https://linkinghub.elsevier.com/retrieve/pii/C20140042396 doi:10.1016/C2014-0-04239-6

21. Alvi JZ, Guan Z, Imran M. Thermoeconomic Evaluation and Sustainability Insights of Hybrid Solar–Biomass Powered Organic Rankine Cycle Systems: A Comprehensive Review. Biomass. 2024 Oct 22;4(4):1092–121. doi:10.3390/biomass4040061

22. Tyagi VV, Rahim NAA, Rahim NA, Selvaraj JAL. Progress in solar PV technology: Research and achievement. Renew Sustain Energy Rev. 2013 Apr;20:443–61. doi:10.1016/j.rser.2012.09.028

23. Dhyani V, Bhaskar T. A comprehensive review on the pyrolysis of lignocellulosic biomass. Renew Energy. 2018 Dec;129:695–716. doi:10.1016/j.renene.2017.04.035

24. Al-Ismaily S, Lal R, Kuzyakov Y, Chorover J, Ba Abood F, Al Maghatasi B, et al. Biochar raises soil health and reduces greenhouse gas emissions in arid lands. Front Soil Sci. 2026 Feb 12;6:1740397. doi:10.3389/fsoil.2026.1740397

25. Woolf D, Amonette JE, Street-Perrott FA, Lehmann J, Joseph S. Sustainable biochar to mitigate global climate change. Nat Commun. 2010 Aug 10;1(1):56. doi:10.1038/ncomms1053

26. Lagnelöv O. Electric autonomous tractors in Swedish agriculture: a systems analysis of economic, environmental and performance effects [Dissertation]. Uppsala: Swedish University of Agricultural Sciences; 2023. 110 p.

27. Lagnelöv O, Larsson G, Nilsson D, Larsolle A, Hansson PA. Performance comparison of charging systems for autonomous electric field tractors using dynamic simulation. Biosyst Eng. 2020 Jun;194:121–37. doi:10.1016/j.biosystemseng.2020.03.017

28. Tumuluru JS, Tabil LG, Song Y, Iroba KL, Meda V. Grinding energy and physical properties of chopped and hammer-milled barley, wheat, oat, and canola straws. Biomass Bioenergy. 2014 Jan;60:58–67. doi:10.1016/j.biombioe.2013.10.011

29. Niedziółka I, Szpryngiel M, Kachel-Jakubowska M. Assessment of the energetic and mechanical properties of pellets produced from agricultural biomass. Renew Energy. 2015;76:312-7. doi:10.1016/j.renene.2014.11.040

30. Carmen. Straw pellet machines for sale [Internet]. 2025 [cited 2026 Mar 9]. Available from: https://www.richipelletmachine.com/straw-pellet-machine-for-sale/

31. Richi Manufacture. Straw Pellet Machine [Internet]. 2025 [cited 2026 Apr 23]. Available from: https://www.richipelletmachine.com/straw-pellet-machine-for-sale/

32. RichenTek. Wheat Straw Pellet Mill [Internet]. 2025 [cited 2026 Apr 23]. Available from: https://www.smallpelletmachine.com/application/wheat-straw-pellet-mill/

33. Kalam A, King A, Moret E, Weerasinghe U. Combined heat and power systems: economic and policy barriers to growth. Chem Cent J. 2012 Dec;6(S1):S3. doi:10.1186/1752-153X-6-S1-S3

34. Fröling Heizkessel. CHP [Internet]. 2026 [cited 2026 Jan 15]. Available from: https://www.froeling.com/en-cz/products/heat-and-electricity/chp/

35. Su W, Li L, Wang L, Ma C, Wang C, Ren X, et al. Improving the Flexibility of Combined Heat and Power (CHP) Units by the Integration of Molten Salt Thermal Energy Storage. Energies. 2025 Dec 17;18(24):6595. doi:10.3390/en18246595

36. Xu B, Oudalov A, Ulbig A, Andersson G, Kirschen DS. Modeling of Lithium-Ion Battery Degradation for Cell Life Assessment. IEEE Trans Smart Grid. 2018 Mar;9(2):1131–40. doi:10.1109/TSG.2016.2578950

37. Laakso E, Efimova S, Colalongo M, Kauranen P, Lahtinen K, Napolitano E, et al. Aging mechanisms of NMC811/Si-Graphite Li-ion batteries. J Power Sources. 2024 Apr;599:234159. doi:10.1016/j.jpowsour.2024.234159

38. Wilfred MA, Alkasim A, Timtere P. Comparative evaluation of sodium nitrate, potassium nitrate, and solar salt as phase change materials for latent thermal energy storage in solar electricity generation in North-Eastern Nigeria. World J Adv Res Rev. 2026 Feb 28;29(2):1570–9. doi:10.30574/wjarr.2026.29.2.0432

39. ROCKWOOL. ProRoX PS 965 [Product Datasheet] [Internet]. 2024 [cited 2026 Feb 4]. Available from: https://brandcommunity.rockwool.com/asset/faxL9NHqtwbxCGLWqE5wOA/asset.pdf?quality=10

40. Incropera FP, Dewitt DP. Fundamentals of Heat and Mass Transfer [Internet]. 6th ed. New York: Wiley; 2006 [cited 2026 Feb 14]. Available from: https://drive.google.com/file/d/0By3v7l7c0TJNZWM5YjNiOGYtOTg1OS00ODYyLWJjZmUtZDA2YTYwYjM3MWZk/view?resourcekey=0-x_AHOIJoV3aPCc2RdZbTPA

41. Oller Westerberg A, Lindahl J. National Survey Report of PV Power Applications in Sweden [Internet]. International Energy Agency; 2022 [cited 2025 Feb 6]. Available from: https://iea-pvps.org/wp-content/uploads/2022/10/National-Survey-Report-of-PV-Power-Applications-in-Sweden-2021.pdf

42. SMHI. Ladda ner meteorologiska observationer [Internet]. Stockholm: SMHI; [cited 2025 May 6]. Available from: https://www.smhi.se/data/hitta-data-for-en-plats/ladda-ner-vaderobservationer/irradiance/98735

43. European Commission. Photovoltaic Geographical Information System (PVGIS) [Internet]. European Commission; 2025 [cited 2026 Jan 25]. Available from: https://re.jrc.ec.europa.eu/pvg_tools/en/

44. Yu FW, Chan KT, Sit RKY, Yang J. Review of Standards for Energy Performance of Chiller Systems Serving Commercial Buildings. Energy Procedia. 2014;61:2778–82. doi:10.1016/j.egypro.2014.12.308

45. Ferreira Junior WN, Resende O, Oliveira DCD, Oliveira DECD, Rosa EDS. Estimating energy efficiency of the aeration process of stored grains through machine learning. Rev Bras Eng Agríc E Ambient. 2024 Nov;28(11):e281001. doi:10.1590/1807-1929/agriambi.v28n11e281001

46. Aboelela D, Saleh H, Attia AM, Elhenawy Y, Majozi T, Bassyouni M. Recent Advances in Biomass Pyrolysis Processes for Bioenergy Production: Optimization of Operating Conditions. Sustainability. 2023 Jul 19;15(14):11238. doi:10.3390/su151411238

47. Bridgwater AV. Review of fast pyrolysis of biomass and product upgrading. Biomass Bioenergy. 2012 Mar;38:68–94. doi:10.1016/j.biombioe.2011.01.048

48. Gracia-Monforte C, Lete A, Marias F, Ábrego J, Arauzo J. Energy, exergy and mass balances of a biomass pyrolysis pilot plant. Energy Convers Manag. 2026 Apr;353:121154. doi:10.1016/j.enconman.2026.121154

49. De Oliveira E Silva G, Hendrick P. Photovoltaic self-sufficiency of Belgian households using lithium-ion batteries, and its impact on the grid. Appl Energy. 2017 Jun;195:786–99. doi:10.1016/j.apenergy.2017.03.112

50. Anderist Rangel Y, Fägerlind K, Ländell G. Improvements in agrienvironmental and grassland statistics in Sweden [Report]. Stockholm: Statistics Sweden (SCB); [2016].

Acknowledgements

I want to thank my family for providing me with discipline and love through hard times; it means more than anything. Finally, my deepest gratitude to my supervisor, Gunnar Larsson, who has shown me nothing but uncompromised kindness, expertise, and support.

Appendix 1

Scenario 1
Biomass results from Scenario 1 (Baseline) simulation

A.1 Biomass

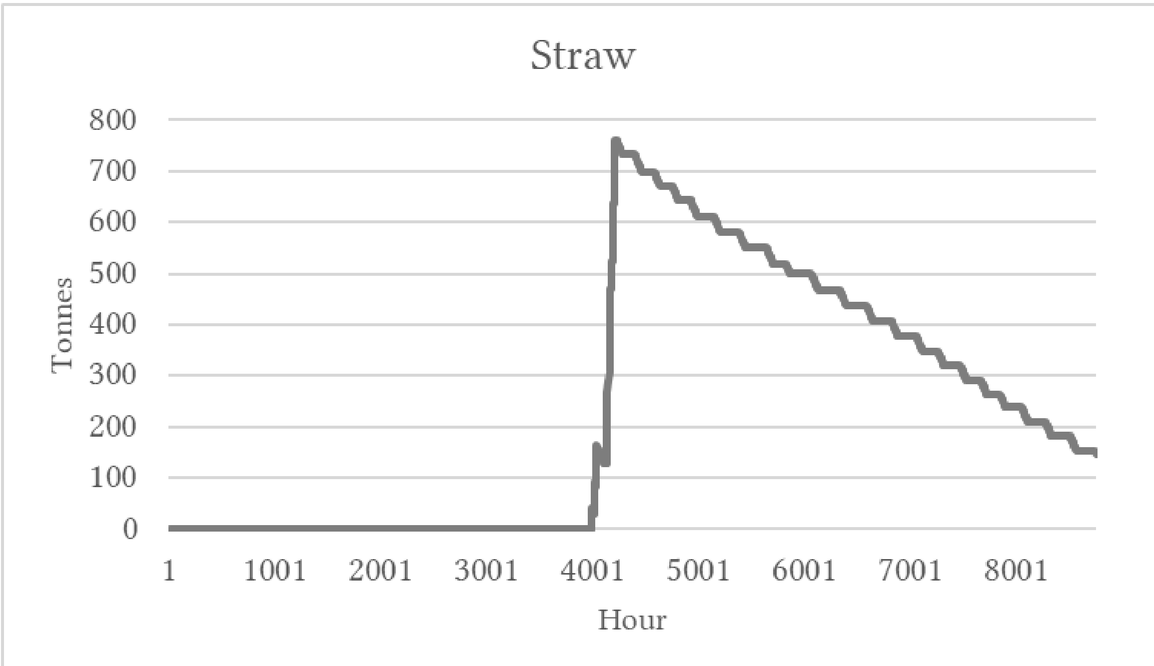

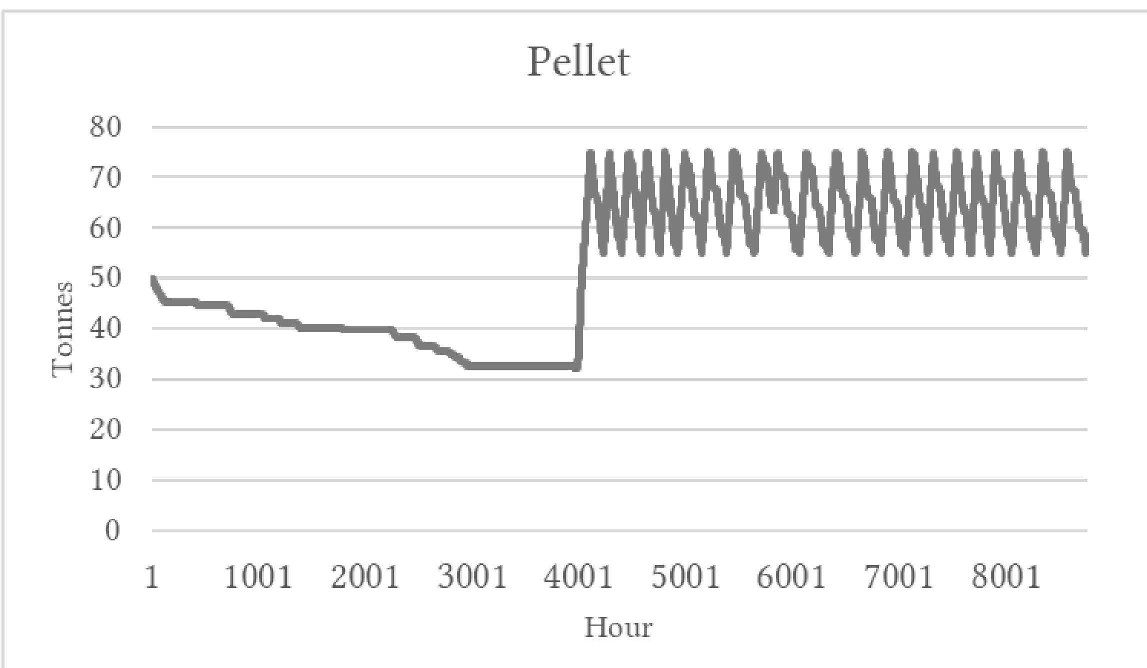

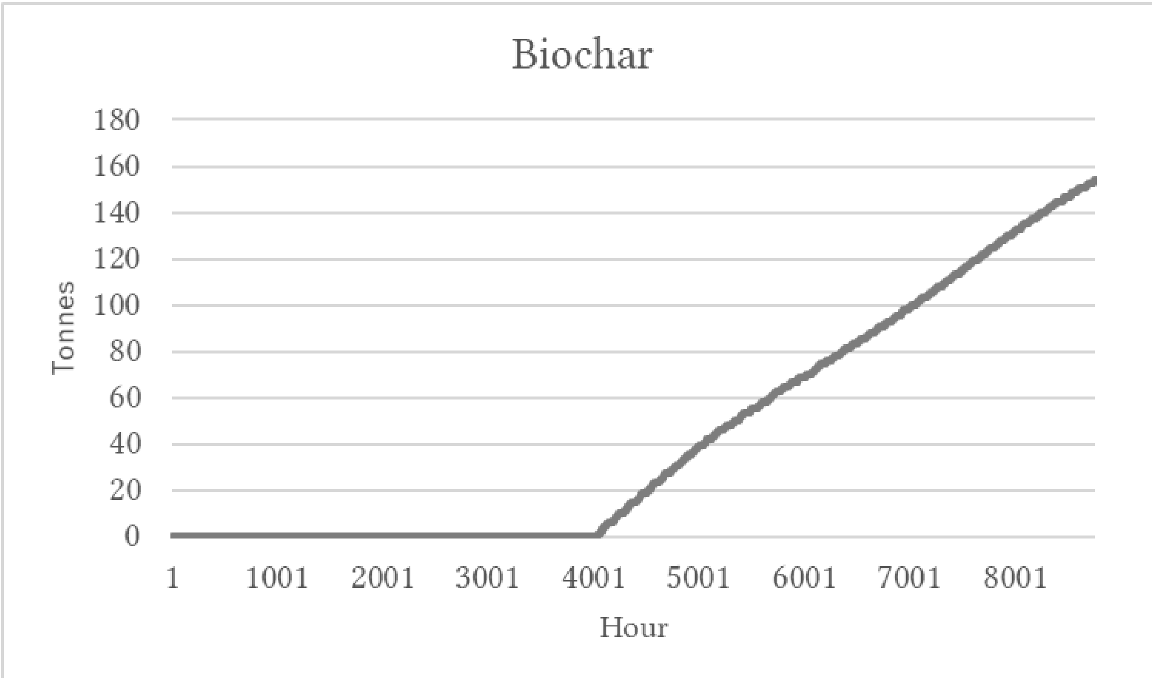

End of year supply [Tonnes]	
Straw	Biochar
147,8	154,3

Appendix 2

Scenario 2
Biomass results from scenario 2 (Non-TES) simulation

A.2 Biomass

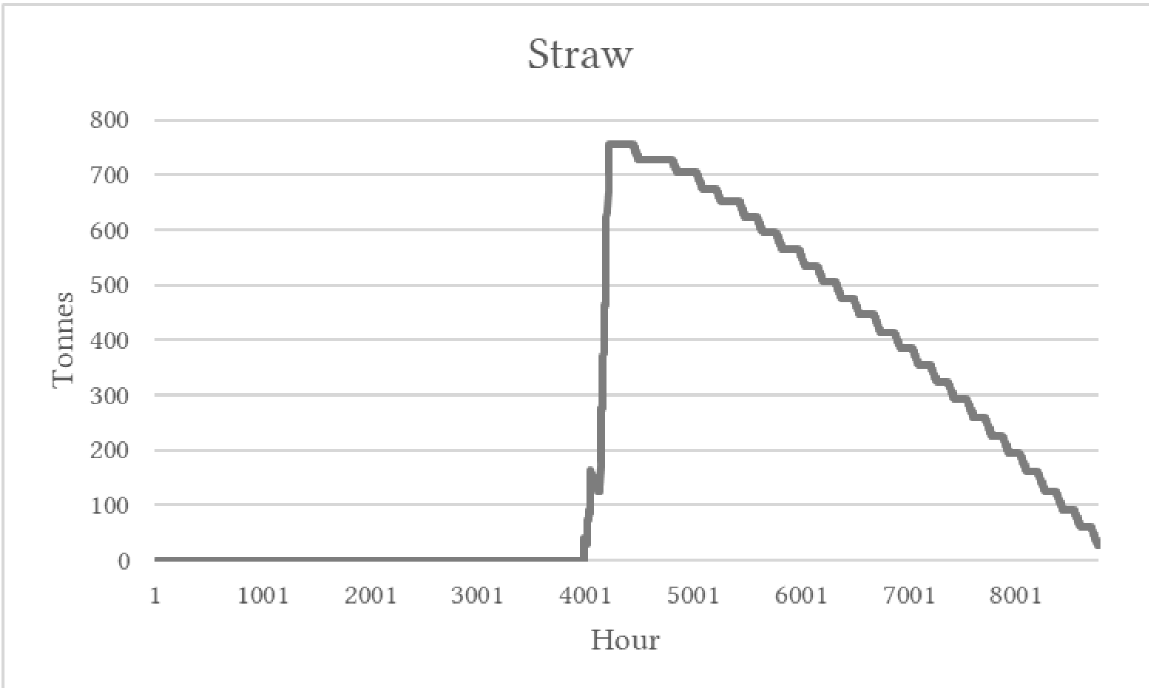

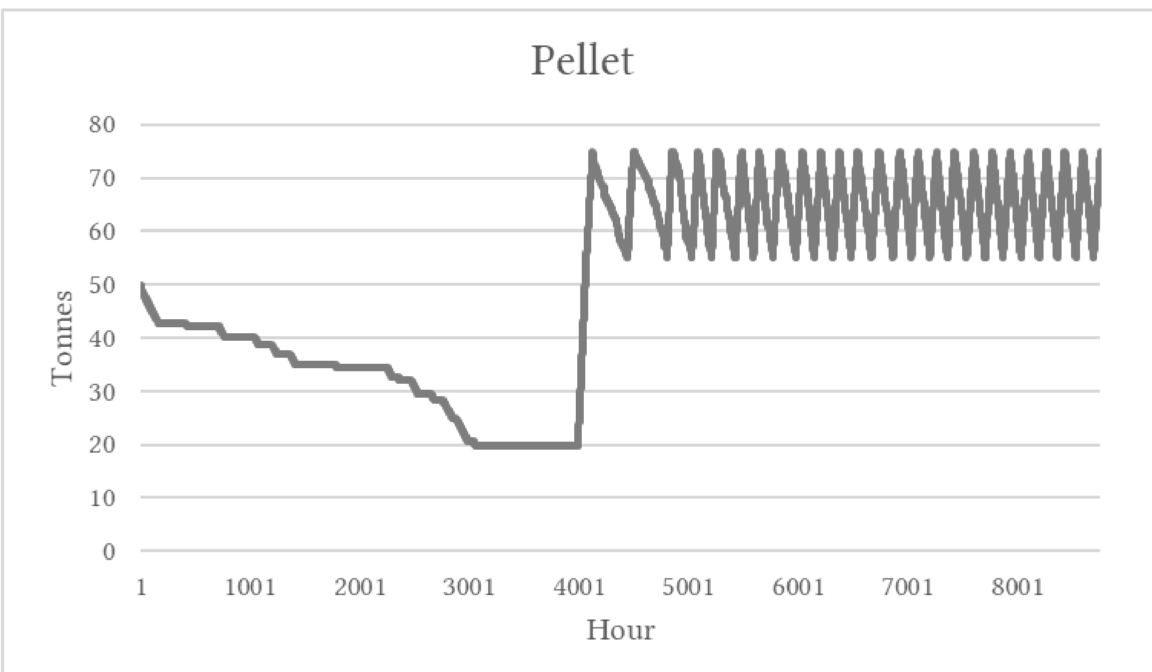

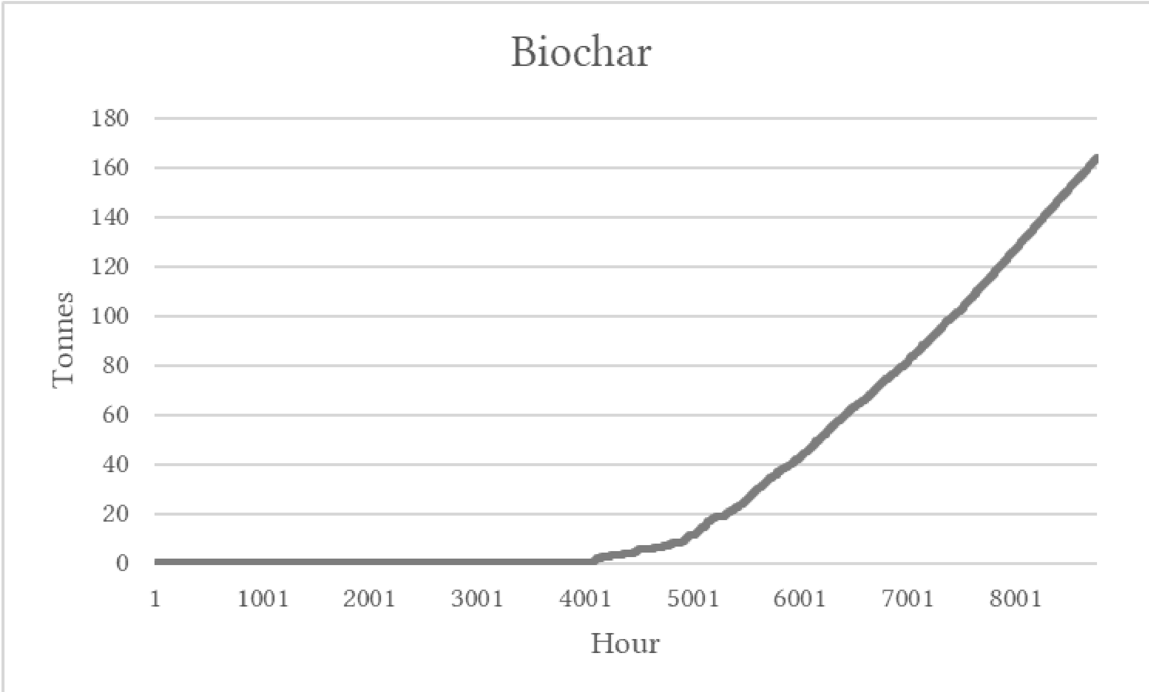

End of year supply [Tonnes]	
Straw	Biochar
26,9	164,1

Appendix 3

Matlab codes used in the simulations

settingsErik_Q1.m:

```
function [arrayRunInput] = settingsErik_Q1(m_aAll)
%The script is executed to set variables for running the simulations. It consists of two parts:
%The first part sets variables that are usually unchanged between
%simulations.
%The second part sets variables that are changed between simulations.
% --- Invärden, statiska ---
%fEfficiency=1;        %Verkninsgrad på laddning/urladdning på batteri
control=struct( ...
  "bUsePV",1, ...              %Inga solceller
  "drivers",99, ...            % Number of tractor drivers
  "bWaitInField",1);           % If the tractor should wait in the field if the conditions are no longer driveable (too much rain) or
the working day is finished
timing=struct(...
  "WorkingHours",10, ...   % Antalet timmar som arbetas, 24 för full autonomi, 10 för normal diesel.
  "MidDayBreak_h",0);      %Om tar hänsyn till arbetstiden vanligen inte är allt i sträck utan även har ett avbrott mitt på dagen
%Variabler som kan ändra för körningar, men som för närvarande har ett
%visst värde
tractor=struct(...
    "items",2, ...         % No of tractors
    "fuel",2, ...          % Batteribytarsystem
    "mass_kg",10550);      % Mass of tractor
%For fuel:
% 1=El (laddning med batteri i fordonet)
% 2=El (batteribytessystem)
% 3=Diesel miesel
% 4=H2 (i bränslecell)
battery=struct( ...
  "items",3, ...               % No of batteries
  "Degradation",1, ...         % Om batteriet åldras. 1=nej, 2=ja. Diesel/H2, alltid 1.
  "CyclesIn",0);               % Start antal cykler, aktiveras i modellen.
% Övriga indata Erik modell
Erik=struct( ...
  "PV_area",200, ...           % Area of PV cells
  "NrCHP",1);
%
charging=struct( ...
  "rate_kW",3960, ...               %Size of chargers
  "items",1, ...                    %No of chargers
  "type",2, ...                     %=1 om variabel laddningseffekt, =2 om konstant laddningseffekt. 2 är standard.
  "changingstations",1, ...         %No of changing stations
  "fEfficiency",1);                 %Verkninsgrad på laddning/urladdning på batteri
% Startvärden för gårdens energilager (Erik)
StartState=struct( ...
  "Pellet_kg", 50000, ...
  "ES_Battery", 500, ...
  "TES_kWh", 10000, ...
  "BES_supply_kW", 0 ,...
  "Grid_kWh", 0, ...
  "Tot_BES_supply_kWh", 0, ...
  "CHP_kWh", 0, ...
  "Stirling_kWh", 0, ...
  "Char_kg", 0, ...
  "StrawStorage", 0, ...
  "PV_kWh", 0);
```

```
weather.Weather_crit=3;           %:1:5 %criterium for workability, 3=deToro
breaks=struct( "alwaysexecute",true,...
  "bResilience",false);
%Variabler som ska ändras under simuleringen
%Skapar vektorer med de värden som de ska simuleras över
arrayTractorPower_kW=190;      %[100 150 190];   %Power of tractor
arrayBatterySizes_kWh=270;     %[270 540 1082];
%ex Solcell [100 200 300]
arrayYears=2010;               % Bestäm år för simuleringen (1989-2016) (SOL: 2005-2016) (Nederbörd: 1989-2016) (Temp:
2009-2016)
arraySeasons=1:4;              % 1=winter 2=spring, 3=summer, 4=autumn

totRuns=length(arrayBatterySizes_kWh)*length(arrayTractorPower_kW)*length(arrayYears)*length(arraySeasons)
arrayRunInput=cell(totRuns,1);
iRun=0;
for fBatteryCapacity=arrayBatterySizes_kWh
  battery.capacity_kWh=fBatteryCapacity
  for fTractorPower_kW=arrayTractorPower_kW
    tractor.power_kW=fTractorPower_kW;
    for iYear=arrayYears
      timing.iYear=iYear;
      for iSeason=arraySeasons
        timing.iSeason=iSeason;
        iRun=iRun+1;
        run=struct( ...
          "battery",battery, ...
          "charging",charging, ...
          "control",control, ...
          "timing",timing, ...
          "tractor",tractor, ...
          "weather",weather, ...
          "breaks",breaks, ...
          "StartState", StartState, ...
          "Erik", Erik);
        arrayRunInput{iRun}=run;
      end
    end
  end
end
End
```

ExecuteAll_Q1.m:

```
function [arrayRuns,tblRuns,arrayYearProfiles]=ExecuteAll_Q1(txtFilenameSavedRuns,iStartRun,iEndRun)
txtWeatherDataFile="mAll.mat",functionInput=@settingsErik_Q1;
% Check if the file exists in the current directory
%if not(exist('.gitignore', 'file') == 2)
%    error('You are not executing the program from the right folder!');
%end
%Slumpnummer, används bara för att minska risken att körningar skriver över
%varandras resultat (används då resultaten sparas ner i en .csv-fil efter varje simulering)
currentTime = datetime('now', 'TimeZone', 'local', 'Format', 'yyyy-MM-dd_HH-mm-ss');
% Convert to string
executionid = char(currentTime);
load(txtWeatherDataFile,"m_aAll");          % Load weather data
if nargin>2
  [arrayRuns] = load(txtFilenameSavedRuns);
else
  [arrayRuns] = functionInput(m_aAll);
  txtFilename=strjoin({'input',num2str(executionid)},'_');
  save(txtFilename,'arrayRuns');
end
iRuns=length(arrayRuns);
%Räknare som används resultaten sparas ner i fil.
% Creates a matrix filled with zeros. The matrix has the same number of
% rows as there are years in the array and it has three columns, one per season. The matrix will later contain the start hour and
end hour of the season (based on the number of the hour in a full year, i.e. a number between 1 and 8760).
 candriveatalltimes=ones(8760,1);
if (nargin<2) %if not supplying arguments for start and end set to use all runs
  iStartRun=1
  iEndRun=iRuns
end
Startofyear= struct('ES_Battery', 500, 'TES_kWh', 10000, 'Pellet_kg', 50000, 'Grid_kWh', 0, 'Tot_BES_supply_kWh', 0,
'CHP_kWh', 0, 'Stirling_kWh',0, 'PV_kWh',0, 'Char_kg', 0, 'StrawStorage' ,0);
EndState=Startofyear;
iYearRun=0;
temporalprofiles=cell(iEndRun+1-iStartRun,1);
profilefieldnames={'ES_Battery', 'TES_kWh', 'Pellet_kg','Grid_kWh','Tot_BES_supply_kWh','CHP_kWh', 'Stirling_kWh',
'PV_kWh', 'Char_kg','StrawStorage','Grid_kW','CHP_kW','Stirling_kW','PV_kW'...
  'Pelletizer_kW','Charger_kW','Climate_kW','Heater_kW','CHP_Heat','Heater','Stirling_Heat_Sink','Pyro_Sink','Heat_Loss'};
%profilefieldnames={'charging','driveable','atfields','fromfields','tofields','FinshedFields_ha'};
iProfileFieldnames=length(profilefieldnames);
arrayYearProfiles=cell((iEndRun+1-iStartRun)/4,1);
arrayWithBreaks=[];
arrayWithoutBreaks=[];
bHasBreaks=false;
for iRun=iStartRun:iEndRun
  iRun
  battery=arrayRuns{iRun}.battery;
  charging=arrayRuns{iRun}.charging;
  tractor=arrayRuns{iRun}.tractor;
  timing=arrayRuns{iRun}.timing;
  weather=arrayRuns{iRun}.weather;
  control=arrayRuns{iRun}.control;
  breaks=arrayRuns{iRun}.breaks;
  StartState=arrayRuns{iRun}.StartState;
  Erik=arrayRuns{iRun}.Erik;
  if (breaks.alwaysexecute==true)
     arrayWithoutBreaks=[arrayWithoutBreaks;iRun];
  else
     bHasBreaks=true;
     arrayWithBreaks=[arrayWithBreaks;iRun];
```

```
  end
  if (breaks.bResilience && (~breaks.alwaysexecute))
     if (breaks.are_there_outages_during_season)
        plot(control.bArrayNobreakallyear)
        [timing,weather,control] = DataPerYearandSeason(timing,weather,control,m_aAll);
        [output,temporalprofiles{iRun}]=ExecuteModel2(executionid,iRun,battery,charging,tractor,timing,weather,control);
        arrayRuns{iRun}.output=output;
     else
        % use data from other run
        arrayRuns{iRun}.output=arrayRuns{breaks.iWithoutBreaks}.output;
     end
  else
     control.bArrayNobreakallyear=candriveatalltimes;
     [timing,weather,control] = DataPerYearandSeason(timing,weather,control,m_aAll);
     if (timing.iSeason==1)
        EndState=Startofyear;
     end
     EndState %Remember to change model name right !!!below!!!
     [output,temporalprofiles{iRun},
EndState]=ExecuteModel_Q1(executionid,iRun,battery,charging,tractor,timing,weather,control,Erik,EndState); %EndState
     arrayRuns{iRun}.output=output;
     sz = [8761 iProfileFieldnames];
     cellDoubles = repmat({'double'}, iProfileFieldnames,1);
     T2 = table('Size',sz,'VariableTypes',cellDoubles,'VariableNames',profilefieldnames');
     if (timing.iSeason==4)
        iYearRun=iYearRun+1
        for i=1:iProfileFieldnames
           winter=temporalprofiles{iRun-3}.(profilefieldnames{i});
           spring=temporalprofiles{iRun-2}.(profilefieldnames{i});
           summer=temporalprofiles{iRun-1}.(profilefieldnames{i});
           autumn=temporalprofiles{iRun}.(profilefieldnames{i});
           stitched=stitchTimeseries_new(winter,spring,summer,autumn,1,1776,3960,5832);
           arrayYearProfiles{iYearRun}.(profilefieldnames{i}) = stitched;
           T2(:,i)=table(stitched.Data);
        end
        txtFilenameTemporalProfile=strjoin(['results\profiles\',"executionid",executionid,"run",num2str(iRun)],"_");
        txtFilenameTemporalProfile=strjoin([txtFilenameTemporalProfile,'csv'],'.');
        writetable(T2,txtFilenameTemporalProfile);
  txtFilenameSummary=strjoin(["results\run_withoutbreaks",executionid],"_");
  txtFilenameSummary=strjoin([txtFilenameSummary,'csv'],'.');
  tblRunsWithoutbreaks=cellArrayOfStructsToTable(arrayRuns,arrayWithoutBreaks);
  writetable(tblRunsWithoutbreaks,txtFilenameSummary);
  tblRunsWithbreaks=cellArrayOfStructsToTable(arrayRuns,arrayWithBreaks);
  txtFilenameSummary=strjoin(["results\run_breaks",executionid],"_");
  txtFilenameSummary=strjoin([txtFilenameSummary,'csv'],'.');
  writetable(tblRunsWithbreaks,txtFilenameSummary);
  tblRuns={tblRunsWithoutbreaks,tblRunsWithbreaks};
  end
  end
'Finished!!!'
beep; pause(0.3); beep; pause(0.3); beep; pause(0.3); beep; pause(0.3); beep
end
```

ExecuteModel_Q1.m

```
function [result, temporalprofiles, EndState] = ExecuteModel_Q1(executionid, iRun, batteries, charging, tractor, timing,
weather, control, Erik, EndState)
%Denna funktion kör modellen med vissa variabler satta.
%tic och toc nedan bara för att skriva ut hur lång tid simuleringen tog i verkligheten på datorn. Behövs inte egentligen.
tic;
%Simulink-modellen innehåller en del som tar hänsyn till hur batteriet
%åldras. Nedanstående kod anpassar hur den körs, där åldrandet kan beräknas med
%tre olika appoximationer.
if (charging.rate_kW/batteries.capacity_kWh<0.5)
  batteries.C_rate=1;
  elseif (charging.rate_kW/batteries.capacity_kWh>=0.5) && (charging.rate_kW/batteries.capacity_kWh<2)
  batteries.C_rate=2;
  else
  batteries.C_rate=3;
end
txtModelname="OscarsModel_Erik_year_Q1";
arrayFieldSizes_ha=[10 16 20 13 15 26 6 14 22 28 17 13];
%Set different inputs for the model
disp(txtModelname)
simIn = Simulink.SimulationInput(txtModelname);
simIn = simIn.setVariable('BatterySize_kWh', batteries.capacity_kWh);
simIn = simIn.setVariable('BatteryNo', batteries.items);
simIn = simIn.setVariable('iChargingModel', 1);
simIn = simIn.setVariable('ChangingStationsNo', charging.changingstations);
simIn = simIn.setVariable('ChargingRate_kW', charging.rate_kW);
simIn = simIn.setVariable('ChargerNo', charging.items);
simIn = simIn.setVariable('ChargerVariableChoice', charging.type);
simIn = simIn.setVariable('CyclesIn', batteries.CyclesIn);
simIn = simIn.setVariable('C_rate', batteries.C_rate);
simIn = simIn.setVariable('iDrivers', control.drivers);
simIn = simIn.setVariable('Degradation', batteries.Degradation);
simIn = simIn.setVariable('fStartBatteryCapacity_kWh', batteries.capacity_kWh);
simIn = simIn.setVariable('Fuel', tractor.fuel);
simIn = simIn.setVariable('fEfficiency', charging.fEfficiency);
simIn = simIn.setVariable('iMaxBreakHours', timing.iMaxBreakHours);
simIn = simIn.setVariable('MidDayBreak_h', timing.MidDayBreak_h);
simIn = simIn.setVariable('m_pStart', weather.m_pStart);
simIn = simIn.setVariable('NrCHP', Erik.NrCHP);
simIn = simIn.setVariable('bNoBreak', control.bArrayNoBreak);
simIn = simIn.setVariable('PV_Area', Erik.PV_area);
simIn = simIn.setVariable('Q_pTableThisYear', weather.Q_pTableThisYear);
simIn = simIn.setVariable('TractorPower_kW', tractor.power_kW);
simIn = simIn.setVariable('TractorMass_kg', tractor.mass_kg);
simIn = simIn.setVariable('WaitInField', control.bWaitInField);
if (control.bUsePV)
  simIn = simIn.setVariable('pvTableThisYear', weather.pvTableThisYear);
  simIn = simIn.setVariable('TempTableThisYear', weather.TempTableThisYear);
end
simIn = simIn.setVariable('RelYear', timing.RelYear);
simIn = simIn.setVariable('iSeason', timing.iSeason);
simIn = simIn.setVariable('iSeasonStart', timing.iSeasonStart_h);
timing.iSeasonEnd_h-timing.iSeasonStart_h
simIn = simIn.setVariable('iSeasonLength', timing.iSeasonEnd_h-timing.iSeasonStart_h+1);
simIn = simIn.setVariable('TractorNo', tractor.items);
```

```
simIn = simIn.setVariable('Weather_crit', weather.Weather_crit);
simIn = simIn.setVariable('WorkingHours', timing.WorkingHours);
simIn = simIn.setVariable('StartState_TES', EndState.TES_kWh);
simIn = simIn.setVariable('StartState_Pellet_kg', EndState.Pellet_kg);
simIn = simIn.setVariable('StartState_ES_Battery', EndState.ES_Battery);
simIn = simIn.setVariable('StartState_Grid_kWh', EndState.Grid_kWh);
simIn = simIn.setVariable('StartState_BES_supply_kWh', EndState.Tot_BES_supply_kWh);
simIn = simIn.setVariable('StartState_CHP_kWh', EndState.CHP_kWh);
simIn = simIn.setVariable('StartState_Stirling_kWh', EndState.Stirling_kWh);
simIn = simIn.setVariable('StartState_PV_kWh', EndState.PV_kWh);
simIn = simIn.setVariable('StartState_Char_kg', EndState.Char_kg);
simIn = simIn.setVariable('StartState_StrawStorage', EndState.StrawStorage);
if (batteries.items<tractor.items)
  error("Number of 'batteries' cannot be fewer than the number of tractors!")
end
SimOut=sim(simIn)                                    %The actual simulation
toc;
strFilename=strcat('results\simulationresults_',executionid)
save(strFilename);
%Lägg resutatet som en rad i lista över alla körningar (med både indata och
%resultat)
timesteps_per_hour=nan;
solverType = get_param(txtModelname, 'SolverType');
if strcmp(solverType, 'Fixed-step')
  % Get the fixed step size
  timesteps_per_hour = str2double(get_param(txtModelname, 'FixedStep'));
else
  'timesteps not ok'
end
result=nan
SimOut.ES_Battery
SimOut.TES_kWh
SimOut.Pellet_kg
SimOut.Grid_kWh
SimOut.Tot_BES_supply_kWh
SimOut.CHP_kWh
SimOut.Stirling_kWh
SimOut.PV_kWh
SimOut.Char_kg
SimOut.StrawStorage
% BES Flows
SimOut.Grid_kW
SimOut.CHP_kW
SimOut.Stirling_kW
SimOut.PV_kW
SimOut.Pelletizer_kW
SimOut.Charger_kW
SimOut.Climate_kW
SimOut.Heater_kW
%Tes Flows
SimOut.CHP_Heat
SimOut.Heater
SimOut.Stirling_Heat_Sink
SimOut.Pyro_Sink
SimOut.Heat_Loss
temporalprofiles=struct('ES_Battery',SimOut.ES_Battery, 'TES_kWh', SimOut.TES_kWh, 'Pellet_kg', SimOut.Pellet_kg,
'Grid_kWh', SimOut.Grid_kWh, 'Tot_BES_supply_kWh',SimOut.Tot_BES_supply_kWh, 'CHP_kWh', SimOut.CHP_kWh, ...
  'Stirling_kWh',SimOut.Stirling_kWh, 'PV_kWh', SimOut.PV_kWh, 'Char_kg', SimOut.Char_kg,
'StrawStorage',SimOut.StrawStorage,'Grid_kW',SimOut.Grid_kW,'CHP_kW',SimOut.CHP_kW,'Stirling_kW',SimOut.Stirling_k
W,'PV_kW',SimOut.PV_kW,...
```

```
'Pelletizer_kW',SimOut.Pelletizer_kW,'Charger_kW',SimOut.Charger_kW,'Climate_kW',SimOut.Climate_kW,'Heater_kW',SimO
ut.Heater_kW, 'CHP_Heat',SimOut.CHP_Heat,'Heater',SimOut.Heater,'Stirling_Heat_Sink',SimOut.Stirling_Heat_Sink,...
  'Pyro_Sink',SimOut.Pyro_Sink,'Heat_Loss',SimOut.Heat_Loss);
EndState= struct('ES_Battery', SimOut.ES_Battery.Data(end), 'TES_kWh', SimOut.TES_kWh.Data(end), 'Pellet_kg',
SimOut.Pellet_kg.Data(end),'Grid_kWh', SimOut.Grid_kWh.Data(end),
'Tot_BES_supply_kWh',SimOut.Tot_BES_supply_kWh.Data(end),'CHP_kWh',SimOut.CHP_kWh.Data(end),
'Stirling_kWh',SimOut.Stirling_kWh.Data(end),'PV_kWh',SimOut.PV_kWh.Data(end), 'Char_kg',SimOut.Char_kg.Data(end),
'StrawStorage',SimOut.StrawStorage.Data(end));
Simulink.sdi.clear
```

stitchTimesseries_new.m:

```
function [ts_full_year_low_res] = stitchTimeseries_new(winter_ts, spring_ts, summer_ts, autumn_ts, winter_start_hour,
spring_start_hour, summer_start_hour, autumn_start_hour)
  % Total hours in a year
  total_hours = 8760;

  % INITIALIZATION FIX: Initialize with NaN instead of 0 to distinguish
  % between "zero energy" and "missing data"
  full_year_data_low_res = nan(total_hours + 1, 1);
  hours_lowres = 0:total_hours;

  ts_full_year_low_res = timeseries(full_year_data_low_res, hours_lowres);

  % Add each season
  ts_full_year_low_res = addSeason(ts_full_year_low_res, winter_ts, winter_start_hour);
  ts_full_year_low_res = addSeason(ts_full_year_low_res, spring_ts, spring_start_hour);
  ts_full_year_low_res = addSeason(ts_full_year_low_res, summer_ts, summer_start_hour);
  ts_full_year_low_res = addSeason(ts_full_year_low_res, autumn_ts, autumn_start_hour);

  % OPTIONAL: Fill NaNs with the last known value to prevent the "drop to zero"
  % ts_full_year_low_res.Data = fillmissing(ts_full_year_low_res.Data, 'previous');
end
function full_ts = addSeason(full_ts, period_ts, start_hour)
  % Pass the entire timeseries object to resample_mean to access time data
  [arrayLowRes, iHours] = resample_mean(period_ts);

  % Ensure we don't exceed the 8761 limit of the full year array
  end_idx = min(start_hour + iHours - 1, 8761);
  data_to_insert = arrayLowRes(1:(end_idx - start_hour + 1));

  full_ts.Data(start_hour:end_idx) = data_to_insert;
end
function [arrayLowRes, iHours] = resample_mean(ts_object)
  % Calculate the actual interval (steps per hour) from the time data
  % Assuming time is in hours. If time is in seconds, divide by 3600.
  time_data = ts_object.Time;
  high_res_data = ts_object.Data;

  % Calculate average steps per hour based on the first two time points
  steps_per_hour = round(1 / (time_data(2) - time_data(1)));

  l = length(high_res_data);
  iHours = floor(l / steps_per_hour);
  arrayLowRes = zeros(iHours, 1);

  for i = 1:iHours
    low = (i-1) * steps_per_hour + 1;
```

```
        high = i * steps_per_hour;

        % Calculate the mean for this hourly bucket
        arrayLowRes(i) = mean(high_res_data(low:high));
    end
End
```

DataPerYearandSeason.m:

```
function [timing,weather,control] = DataPerYearandSeason(timing,weather,control,m_aAll)
StartYearMostData=1989;     % First year for percipitation data
StartYearSun=2005;          % First year for solar radiation data is 2005 and for Temp it is !!!2009!!!
StartYearTemp=2009;
if ((timing.iYear<1989) || (timing.iYear>2018))
  error('Years must be in the interval 1989-2018.');
end
%Years relative to start of data
RelYear=timing.iYear-StartYearMostData+1;
RelYearSun=timing.iYear-StartYearSun+1;
RelYearTemp=timing.iYear-StartYearTemp+1;
%nederbördstabell
Q_pTable=readtable('Percipitation.xlsx');
%tabell över solelseffekter
if (control.bUsePV)
   pvTable=readtable('Sun.xlsx','Sheet','Data');
   pvTable=table2array(pvTable);
   disp(length(pvTable))
   pvTableThisYear=pvTable(:,RelYearSun+1);
   TempTable=readtable('TempC_2009-2016_edited.xlsx', 'Sheet','TempC_2009-2016'); %Arlanda_lufttemp_2023_samma
   TempTable=table2array(TempTable);
   disp(length(TempTable))
   TempTableThisYear=TempTable(:,RelYearTemp+1);
else
   pvTableThisYear=[0 0];
end
Q_pTableThisYear=Q_pTable{:,RelYear+1};
Q_pTableThisYear(1)=[];
Starthours=[1 1776 3960 5832];
Endhours=[1775 3959 5831 8760];
iRemoveTill=Starthours(timing.iSeason);
if (iRemoveTill>0)
   Q_pTableThisYear(1:iRemoveTill-1776)=[];
   hours2=length(Q_pTableThisYear);
   weather.Q_pTableThisYear=[(1:hours2)' Q_pTableThisYear];
   if (control.bUsePV)
       pvTableThisYear(1:iRemoveTill)=[];
       hours=length(pvTableThisYear);
       weather.pvTableThisYear=[(1:hours)' pvTableThisYear];
       TempTableThisYear(1:iRemoveTill)=[];
       weather.TempTableThisYear=[(1:hours)' TempTableThisYear];
   end
end
timing.RelYear=RelYear;
timing.iSeasonStart_h=Starthours(timing.iSeason);
timing.iSeasonEnd_h=Endhours(timing.iSeason);
control.bArrayNobreakallyear=control.bArrayNobreakallyear(timing.iSeasonStart_h:8760);
l=length(control.bArrayNobreakallyear);
control.bArrayNoBreak=[(1:l)' control.bArrayNobreakallyear];
%Max number of hours during a season
timing.iMaxBreakHours=Endhours(timing.iSeason)-Starthours(timing.iSeason);
```

```
if (timing.iSeason==1)
  weather.m_pStart=100000
else
  weather.m_pStart=m_aAll(timing.iSeasonStart_h-1775,timing.RelYear);
end
end
```

Publishing and archiving

Approved students' theses at SLU can be published online. As a student you own the copyright to your work and in such cases, you need to approve the publication. In connection with your approval of publication, SLU will process your personal data (name) to make the work searchable on the internet. You can revoke your consent at any time by contacting the library.

☐ YES, I, Erik Guldevall, have read and agree to the agreement for publication and the personal data processing that takes place in connection with this

☐ NO, I/we do not give my/our permission to publish the full text of this work. However, the work will be uploaded for archiving and the metadata and summary will be visible and searchable.